Measurement Light Bulb

EE3L11
Electrical Engineering Bachelor Thesis

Subgroup:
Power distribution, motors and construction

Authors:
S.O. Jordan (s.o.jordan@student.tudelft.nl)
I. van der Werf (i.vanderwerf@student.tudelft.nl)

Supervisors:
Prof. Dr. E. Eisemann
Dr. M. Billeter
N. Salamon

July 25, 2019

DELFT UNIVERSITY OF TECHNOLOGY

FACULTY OF ELECTRICAL ENGINEERING, MATHEMATICS
AND COMPUTER SCIENCE

ELECTRICAL ENGINEERING PROGRAMME

Abstract

This document describes the design process the prototype of a measurement light bulb which is able to project spherical harmonics of orders 0-1-2. Photographs of these projections can be combined to represent many light distributions. The measurement light bulb can be used in the field of research focused on the computation of the illumination impact of lighting, more specifically, simulating different light sources. Our prototype consists of a laser beam rotating over two axes, which allows the device to project onto a sphere around itself. The device can be controlled wirelessly using Bluetooth.
The lamp can project spherical harmonics in a resolution of 4° and 256 monochrome light levels. The time one projection takes is about one second, which allows for quick measurements. The dimensions and the weight of the lamp are such that it is portable. At this stage, the prototype can only operate in a dark environment, due to the use of a low powered laser.
In this document, the focus will be on the design of the power distribution, the motors and the construction.

Preface

We would like to wholeheartedly thank everyone involved in this project.
Our supervisors Elmar Eisemann, Markus Billeter and Nestor Salamon for giving excellent guidance during this project. They were always compassionate to us and brought excellent knowledge to the table. They also delivered very helpful advice regarding the writing of our theses.
Ioan Lager also receives our gratitude for organising the bachelor graduation project and keeping things on track.
Another person we would like to thank is Jianning Dong, who gave us advice regarding motors and their corresponding controllers.
We would also like to thank the Intelligent Systems Department for letting us use their cluster computer, which allowed us to run a heavy optimisation algorithm for pattern calculations, and letting us use their 3D printer, which allowed us to easily produce custom parts.
Lastly we would like to thank Martin Schumacher for being supportive of our project and his dedication to make sure all our components were delivered in time.

Contents

Chapter 1: Introduction

Almost nothing is as much part of our everyday life as light. It is therefore no surprise that light can have a large impact on us: correct lighting can set the right mood and is thus also an important element in interior design. Designing a room requires knowledge of how the room is to be lit, what it is going to look like and how this influences the people inside. Simulating lighting plays a big part in this. Computer programs have been developed specifically for this purpose. However, simulating light, either from a lamp or from the sun, turns out to be hard, since the way it spreads across a room depends on a large number of factors, a lot of which are unknown. Due to this, computer simulation is very costly and difficult to control. This is where our project comes in.

Instead of simulating lamps via computer programs, we opt for a simulation with a physical measurement light bulb. This measurement light bulb has been built to project a finite set of special light patterns: spherical harmonics (SHs), which can be combined to represent many light distributions.

The principle is to capture the device's illumination impact from a given point in the room with the aid of a camera. The photos, resulting from capturing several spherical harmonics projections from the measurement light bulb, can be combined in a post-process to yield the result that would have been obtained by a different light source placed at the same location. For any light source, a specific combination of SHs coefficients exist so that their weighted linear combination yields an approximation of the light's emission pattern. In consequence, by combining the photos using the same coefficients, we can predict the illumination of the given light source. The resulting technique is a lot more efficient than simulating all reflections of the room.

When the light bulb is able to project high resolution SHs and the reflectance properties can be captured, many sorts of light sources could be simulated. Hereby, our work can become a useful tool for interior designers to simulate lighting in a room, or even an entire building. It is possible to have a preview of the results of lamp arrangements without physically installing these. Hereby, the user saves a lot of time and as the capture is only performed once, it enables the exploration of many design options in a post-process.

In this chapter, some prerequisite knowledge about spherical harmonics will first be discussed. This is followed by a brief overview of some related work. After this, the problem definition is laid out. Next come the criteria for the prototype, an overview of the project dynamics and lastly an outline of the entire thesis.

1.1 Prerequisite knowledge about spherical harmonics

As indicated in the introduction, the idea of our solution is to approximate the light emission pattern of a light source using spherical harmonics and rely on our measurement light bulb to actually emit the spherical harmonics pattern into the scene. In order to provide a better understanding, we will first briefly revisit spherical harmonics.

Spherical harmonics are a set of orthogonal basis functions over a sphere. In principle, they can be thought of as the equivalent of a Fourier basis on a spherical surface. In consequence, they can be used to represent various spherical functions by projecting the function into their spherical harmonics basis. The higher the order of the basis, the more accurate the representation of the function becomes (similar to adding frequencies for the Fourier case).

The general equation for complex spherical harmonics is given in Equation 1.1. However, since complex light cannot be projected, they are transformed to form a real basis.

$$Y_l^m(\theta, \phi) = Ne^{im\phi}P_l^m(cos(\theta)) \tag{1.1}$$

In Equation 1.1, l is the order and m is the index of the spherical harmonic function Y, N is the normalisation constant and P is the Legendre polynomial. ϕ is the longitude and θ the colatitude of the sphere as can be seen in Figure 2.2.

In our work, we will focus on a lower dimensional SH space up to order two (as illustrated in Figure 1.1). In the future, higher order representations could be added, but it has been shown that the first three bands can be used to make very accurate representations [Ramamoorthi and Hanrahan, 2001].

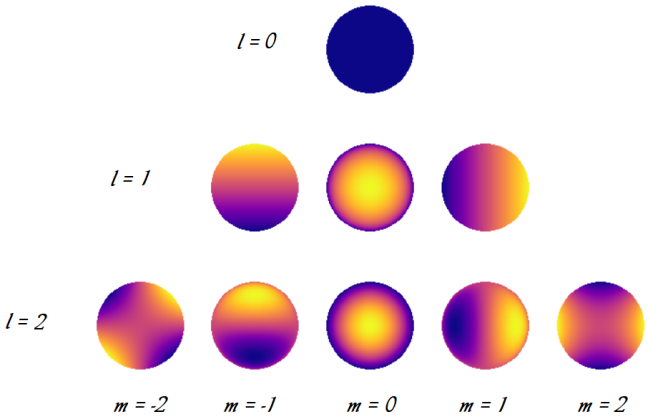

Figure 1.1: The first three order of spherical harmonics. l indicates the order, m the index. Source: [Luger, 2018]

1.2 Related work

The goal of illuminating an environment in a post-process instead of actively setting up lights has received much interest in the past from the vision and graphics community but none focused on building a portable device to support the simulation of arbitrary emission patterns.

For omnidirectional light sources, an algorithm exists, which served as the inspiration for our work. In this case, a lamp is used to sweep the environment, while recording a video. The captured imagery can then be used to relight the scene [Salamon et al., 2017].

Multiple projects study the interaction of light and objects by projecting light from a fixed measurement setup around the object [Debevec et al., 2000; Hawkins et al., 2001; Levoy et al., 2000; Tunwattanapong et al., 2013]. A big disadvantage is that most of these projects require large constructions that are hard to bring to different locations and cannot be used to project outwards into an entire room.

Until now only a couple of projects exist that direct light patterns outward into an entire room. Most of these projects are about screens to be looked at. These screens can take the form of a sphere, or a spinning ring of LEDs that creates an image through persistence of vision (POV) [GreatScott!, 2017; Groenendijk, 2018; Yamada et al., 2017]. While it might seem possible to use such screens as a light source and emit patterns into the room, their light is diffuse and thus does not allow us to derive a clear projection of the displayed pattern to the surroundings.

1.3 Problem definition and challenges beyond previous work

For this project, the aim is to make a portable setup that projects spherical harmonics outward, making it possible to cover an entire room as opposed to just objects. This project differs from the ones in Section 1.2. Firstly, we need an outward projection instead of an inward projection. Secondly, a certain resolution is

required in order to be able to project spherical harmonics, even at varying distances, since not every wall has the same distance to the measurement light bulb.

1.4 Criteria for the prototype

The main criterion for the prototype is that it needs to be able to project spherical harmonics at such an intensity and resolution that the impact of the illumination can be captured by a camera. The photos of these projections can then be used to accurately simulate any light source. This process should be easy and relatively fast, allowing the user to intuitively use this device to simulate lighting options for the room. Another criterion is that the device should be safe to use, portable and cheap, allowing research groups to build one and easily test it out themselves.

1.5 Project dynamics

The project proposer is the Computer Graphics and Visualization (CGV) group, thus the prototype is to be delivered to them. The bachelor graduation project is executed in a group of six people, that is divided into three subgroups of two people. Each subgroup is responsible for a specific part of the project and hands in a corresponding thesis. The distribution of the subgroups is as follows:

- Rob Damsteegt & Jippe van Dunné → control, communication and PCB design
- Sebastian Jordan & Ids van der Werf → power distribution, motors and construction
- Bob van Nifterik & Jurgen Wervers → light sources, the corresponding drivers and camera synchronisation

All of these three theses will cover the project globally and their own subsystems in more depth. The thesis outline given in the next section is therefore specific to this thesis.

1.6 Thesis outline

The next chapters are structured as follows. First, we discuss the design in Chapter 2 and the programme of requirements in Chapter 3. Then the chapters, specific for our subgroup follow. The construction is discussed in Chapter 4. The motors are discussed in Chapter 5. The power distribution is discussed in Chapter 6. Then we will elaborate on the integration of the different parts delivered by each subgroup in Chapter 7. After that we will discuss the functionality of the complete system compared to the programme of requirements in Chapter 8. Finally we will discuss the conclusions, recommendations and future work of this project in Chapter 9.

Chapter 2: Design overview

At first, some different design options were drafted. Of these options, one was chosen. An overview of these design options and the reasoning behind the choice can be read in Appendix A.

In this chapter, an overview of the final design will be given. First a general overview is given, followed by a short breakdown of all the subsystems and their placement on the construction.

2.1 Design

A basic overview of the design is given in Figure 2.1. It consists of a laser which is aimed at a fast spinning mirror, driven by a motor (marked 'M'). This construction is driven by a motor (marked 'B'), which rotates slower, such that a small angular step is taken for each complete rotation of Motor M. This allows the laser beam to turn over two axes and to project onto a sphere around itself, as depicted in Figure 2.2. In this figure the colatitude is indicated by θ and the longitude is indicated by ϕ.

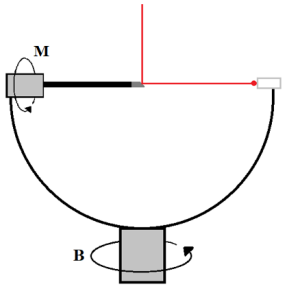

Figure 2.1: Impression of the measurement light bulb design

In this process, the laser 'draws' the spherical harmonics on the walls of the room it is positioned in. Since spherical harmonics contain positive as well as negative values, but 'negative light' does not exist, the positive and negative parts are projected with separate patterns. This can later be compensated for in post-processing.

These projections are captured by a camera, of which the exposure time is controlled to capture an entire projection, so that every part of the room is lit once.

This system is controlled by a microcontroller, which regulates the rotation speeds for both axes, controls the laser and handles communication with the user. This controller, together with some other subsystems, is placed on a printed circuit board (PCB), which is mounted on the moving construction. Power is fed to the system through the lower axle using a slip ring. Control signals for Motor B and the camera are also sent over this slip ring.

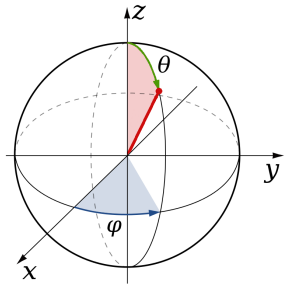

Figure 2.2: Depiction of red laser beam moving over two axes. Source: [Ibrahim]

2.2 System breakdown

The system consists of seven subsystems which are discussed in this section. The location of the subsystems in the final design can be seen in Figure 2.3.

Controller The controller is the one that binds all the subsystems together. It monitors speeds and angles, reads pattern data and converts it to a drive signal for the laser and controls the motors.

Motor M(irror) This motor rotates the mirror. Motor M is implemented with a DC motor and a driver to operate it. The motor as well as its driver are placed upon the moving construction. Attached to the axle of

this motor is the mirror. The driver has a pulse-width modulation (PWM) signal as input, which dictates the speed. The speed of this motor is monitored by a Hall effect switch, which gives a pulse on each rotation.

Motor B(ase) This motor is used to rotate the upper part of the construction. Motor B is implemented with a stepper motor and a driver to operate it. Motor B and its driver are located in the base of the construction and control signals are transmitted from the controller through the slip ring. This slip ring is placed upon the lower axle and the stepper motor is moved off axis and connected with a belt. The stepper motor driver has two inputs, a direction input which determines in which direction it spins and a step input, which makes the motor rotate a step for each pulse sent to it. The speed and orientation of this motor are monitored by a Hall effect switch.

Laser The laser and its driver are also placed upon the moving part. The laser is focused on the mirror using a lens. The laser driver takes a PWM signal as input and produces an accurate drive signal for the laser.

Bluetooth module The Bluetooth module is for connecting the device to for example a phone, which allows the user to control it from a distance. It also enables transmission of pattern data from the user device to the lamp.

Camera The camera is connected to the controller via the slip ring. It is synchronised with the complete system using the microcontroller to make be able to capture exactly one projection with as little noise as possible.

Power supply The power supply is partly on-board and off-board. The on-board power supply contains some voltage regulators, which produce the voltages required for all the different subsystems. This on-board power supply takes a 12 V DC input supplied from the off-board part.

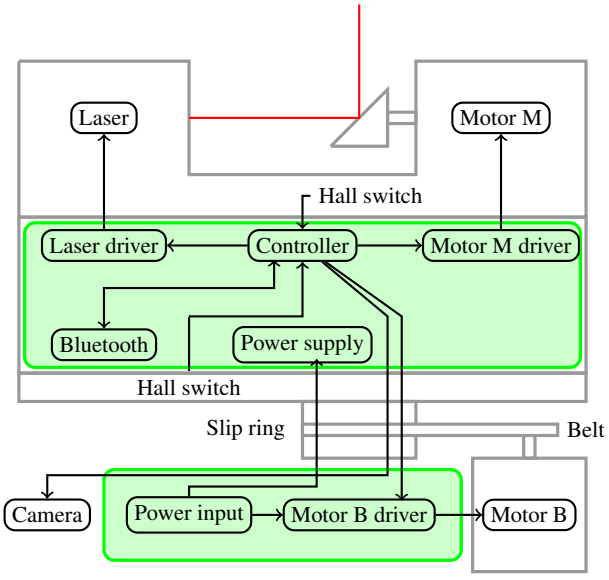

Figure 2.3: Design overview. Circuit boards are depicted by a green frame.

Chapter 3: Requirements for the system

In this chapter, an overview of the requirements of the system is given.

In general, the product should be able to project SHs at a certain light intensity so that the reflections of the pattern can be captured by a camera. The required camera settings are strongly dependent on the type of room, e.g. the amount and direction of lighting in the room. Therefore, the assumptions on the environment in which we aim the product to be working will be specified first. After that, the requirements for the system in order for it to work in the assumed environment will be stated.

3.1 Assumptions on the system and its environment

To be able to simulate lamps, all different light colours need to be simulated. However, we assume that a proof of concept of this device can also be given if the measurement light bulb only projects in one colour. This will not allow for every lamp to be simulated, since only monochromous simulations are possible.

We also assume that the lamp can be tested in a dark environment, in case the lamp is not bright enough to create visible projections in a lit up room. This allows for a proof of concept even if the light source is not powerful enough for projections in daylight.

3.2 System requirements

In Section 1.4, some system criteria for the prototype were specified. In this section, these criteria will be further specified and quantified. First some definitions will be elaborated, followed by the requirements.

Some definitions that are important for understanding the requirements are given below.

Pattern: This is the projection of one spherical harmonic (SH), of which one or multiple photos can be taken.
Measurement: This is a complete set of patterns, which together form a complete picture. For example, one pattern could be an SH of any of the orders that are desired to display. If the first three orders of SHs are displayed, this means 9 (=1+3+5) SHs in one measurement. Since all the SHs require a positive and negative projection (except for order 0), this results in 17 photographs.

The requirements for the system are listed below and in Table 3.1, where they are specified in three categories: must have, should have and could have.

Angular resolution The angular resolution of the projection is defined in degrees. This resolution is the same for both the longitudinal as the latitudinal direction. These values were chosen based on simulations. 15° allows for the SHs to be distinguished, but for an accurate representation, an angular resolution of at least 5° is required. A plot for indication can be seen in Figure 3.1.

Projection time This is the amount of time one pattern projection takes. It is proportional to the resolution and inversely proportional to the speed of the motors. It is required that it takes a finite time to project the pattern correctly, but ideally, this is in the order of a minute or a second.

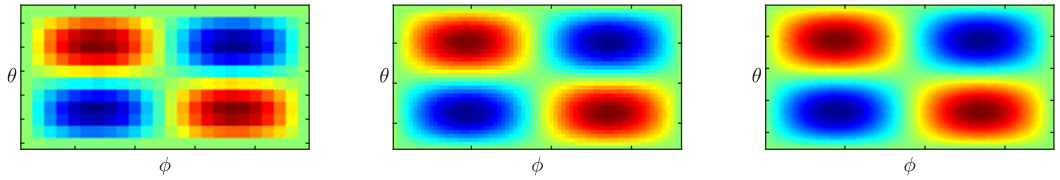

(a) Angular resolution of $15°$ (b) Angular resolution of $5°$ (c) Angular resolution of $2°$

Figure 3.1: Three plots of the spherical harmonic function of order 2, index -1 at different angular resolutions

Power Since portability is a criterion, the choice of the power source is important. The most simple source of power is a regular power outlet, but for more portability, an implementation with a battery would be more suitable.

Start-up time This is the time required between switching on the device and the start of the first pattern projection. This involves spinning up the motors, buffering the projection from the memory and synchronising the system. Between pattern projections, the time required for setup is less, because the motors are kept spinning and only the memory needs to be updated for the next pattern.

Dimensions For better portability, smaller dimensions are preferable. The prototype should fit through a door, so measurements of any room can be taken.

Phase drift Phase drift is the deviation in average speed of the projection over one of the two axes. Ideally this average speed deviation would be zero, because then the pattern does not shift over the sphere. The allowable amount of phase drift is the same for both axes. The values for this are chosen based on the angular resolution, meaning that they are the same amount of degrees per revolution (divided by two, to account for the positive and negative direction of the phase drift).

Maximum phase error This is the maximum phase error of the projection caused by vibrations or instabilities of the system. This means that there can still be a phase error while the phase drift is zero. The maximum phase error is the same for both axes and has the same bounds as the phase drift.

Colour of the light source To simulate any lamp, the projection should contain all colours. However, monochromous design can also suffice for a prototype.

SH orders The more SH orders are projected, the more accurate the resulting computer simulations can be. It is required that at least the SHs up to order two can be projected for simple simulations.

Brightness This involves the power of the light source on the device. The power should at least be high enough to be able to capture projections in a dark room. However, higher power would allow for capturing in brighter environments, ideally in daylight.

Light levels The amount of different light levels contributes to the resolution of the projection. The more light levels, the less quantisation noise occurs in the projection. However, since the camera has $14\,\mathrm{bit}$ light levels, a higher accuracy than this is not visible.

Camera synchronisation For capturing these projections, synchronisation with the camera is desired. This allows the exposure time to contain exactly one pattern projection, which minimises the amount of captured noise light.

User interface For controlling the device, a user interface (UI) is required. Any working UI suffices for the prototype but a graphical UI (GUI) is preferred for a more intuitive experience.

Table 3.1: Overview of complete system requirements

Type	Must have	Should have	Could have
Angular resolution	$15°$	$5°$	$<5°$
Projection time	"converges"	$1\,\mathrm{min\,pattern^{-1}}$	$1\,\mathrm{s\,pattern^{-1}}$
Power	230 V, 16 A	-	battery powered
Start-up time	$<15\,\mathrm{min}$	$<1\,\mathrm{min}$	$<10\,\mathrm{s}$
Dimensions	$1\,\mathrm{m}$ x $1\,\mathrm{m}$ x $1\,\mathrm{m}$	"fits through door" $<0.8\,\mathrm{m}$ for smallest rib	$0.4\,\mathrm{m}$ x $0.4\,\mathrm{m}$ x $0.4\,\mathrm{m}$
Phase drift	$7.5\,°\,\mathrm{rev^{-1}}$	$2.5\,°\,\mathrm{rev^{-1}}$	$<2.5\,°\,\mathrm{rev^{-1}}$
Maximum phase error	$15°$	$5°$	$<5°$
Colour of the light source	monochrome	-	RGBW
SH order	0-1-2	-	higher orders
Brightness	Capturable in completely dark room	-	Visible in daylight
Light levels	8 (3 bit)	256 (8 bit)	16384 (14 bit)
Camera synchronisation	Change settings and take pictures manually	Change settings manually, use microcontroller to take pictures	Everything done by microcontroller
User interface	working UI	-	GUI

Price A requirement that does not have a must/should/could have value is price. However, the goal is to make this prototype relatively cheap, since that makes it accessible to research groups to reproduce and use for themselves.

Safety Safety constraints should also be taken into consideration. Some parts of the light bulb may be moving, which the construction should support. Also, the light bulb needs power. The system that takes power from the mains should be safe and intuitive to use in order to avoid electric shocks or a short circuit. A safety system should be included in the design, so that in case of any failure or danger, the system shuts down by itself.

Chapter 4: Construction

In this chapter we discuss the details about the construction. We will start by identifying the requirements for the construction in Section 4.1. After this we discuss the implementation of the construction by describing the different parts in Section 4.2, and finally we will present and discuss the results of the designed construction in Section 4.3.

4.1 Requirements for the construction

In this section we discuss the requirements for the construction. The only requirement in Chapter 3 that directly concerns the construction, is the requirement for the dimensions of the system. However, we set more detailed requirements for the construction, as listed below. These requirements are all of the category 'Must have' since these must be reached in order to have a working system.

1. The construction should be able to rotate in such a way that the light source can span an entire sphere, apart from the part that is obstructed by the construction itself. This requires two axes of freedom: axis M and axis B.

2. Ideally the construction does not obstruct the projection of the light pattern and its reflections. As the construction has to be somewhere, it will result in some obstruction and our goal is to keep it minimal.

3. The two motors, one for each axis, should be securely mounted in the construction.

4. The distance between the mirror and the light source should be variable, so that the distance from the light source to the mirror can be adjusted to match the focal length of the light beam. Further elaboration is given in Section 4.2.

5. The rotating part of the construction should receive power, since Motor M, the laser and the PCB are on the rotating part of the design, and these need power to operate.

6. Safety constraints should be taken into consideration. The construction must be able to withstand the stress on its materials while operating, with the speeds mentioned in Chapter 5.

4.2 Implementation of the construction

In this section we will elaborate on the implementation of the construction. First an overview of the implementation is given, then parts of the construction will be discussed individually, followed by a discussion about the building material.
An overview of the implemented construction is given in Figure 4.1.

4.2.1 Parts of the implemented construction

In this section we will discuss the different parts of the implemented construction. A visualisation of all the parts is given in Figure 4.1. Technical drawings of all parts can be found in Appendix C.

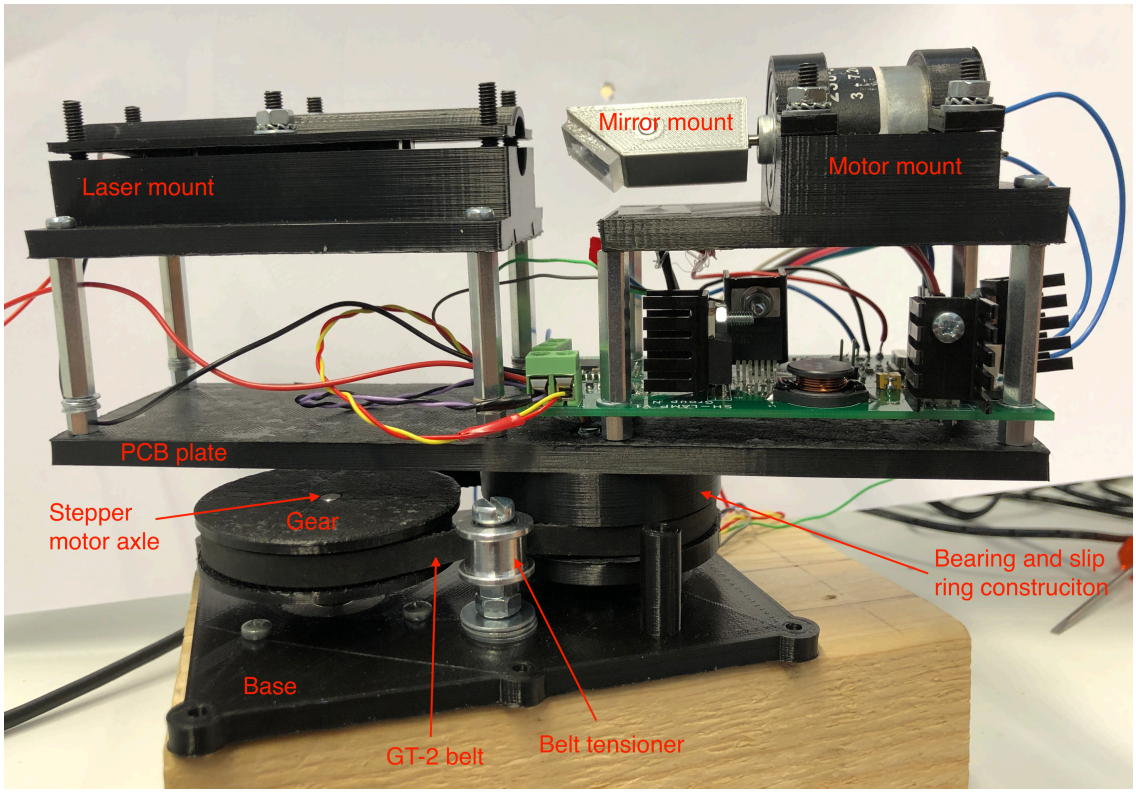

Figure 4.1: Photo of the complete construction with annotations of the different parts.

Mirror mount

The mirror mount is the part that is mounted on the axle of Motor M. The angle of the mirror with respect to the light beam has to be $45°$, to ensure that it spans a circle exactly above the point where the mirror and light beam meet. The second axis can then be aligned through this point in order to let the system span a sphere. The mirror mount has a hole, designed so that the magnet which is used for the motor control (discussed in Chapter 5) fits in. To prevent oscillations during the rotation, the hole for the motor axis is exactly aligned with the centre of mass of the mirror mount. A set screw is used to mount the mirror mount on the motor axle.

Motor M mount

The mount for Motor M should hold this motor in place securely. However, the motor should not be completely covered to prevent it from getting too hot. For this reason two brackets are used to hold the motor in place with a large gap between them. The brackets are tightened by two bolts each and these bolts are countersunk on one side. This motor mount also has a small recess to place a hall effect sensor for speed feedback.

Laser mount

The laser mount is similar to the motor mount, but it has one bracket that is the full length of the mount. This way the laser can be placed anywhere, within the length of the bracket, to make sure the distance of the light source to the mirror coincides with the focal length. When the laser beam is set to a specific opening angle using a lens, the beam will first converge into a point, called the focal point, and will then diverge. This is depicted in Figure 4.2. If this focal point coincides with the mirror, it will seem like all the light from the system originates from one point. By correctly adjusting this focal point, the quality of the projection onto the surroundings is improved, since the laser overlap between different parts of the

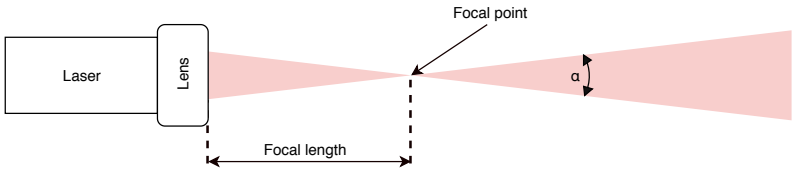

Figure 4.2: Schematic depiction of the focal length of the laser, when it is set to an opening angle (α). The laser beam is depicted in red.

projection does not depend on the distance from the device. Once the laser is in place, it is fixed in this position by tightening six bolts that connect the lower mount and the upper bracket. The laser does not heat up very much, so the fact that the laser is completely covered does not cause a problem.

PCB plate

The PCB will be placed on a plate below the motor mount and the laser mount. The total length on one side needs to be longer than the other side, since the laser mount is longer than the motor mount. Because of this, the PCB plate is asymmetric with respect its axis of rotation. However, there is enough space on the construction to balance the weight of the system once all components have been mounted. The PCB plate is also connected to the slip ring and has a hole to feed the wires through that come from the slip ring. The PCB will be mounted to this plate using PCB spacers. These spacers will also be used between the PCB and the motor mount and between the PCB plate and the laser mount.

Bearing and slip ring construction

The motor mount, the laser mount and the PCB plate are connected to the top part of the slip ring, which is the moving part. However, ideally the slip ring should not support the whole construction. For this reason, a bearing is integrated into the construction, to support the rotating part. An exploded view of the bearing and slip ring construction is shown in Figure 4.3b. The teeth of the gear part are designed to match the dimensions of a GT-2 belt, which will be used to rotate the construction. The flange part is designed to prevent the belt from slipping off the gear part and has a hole for the bearing to fit in.

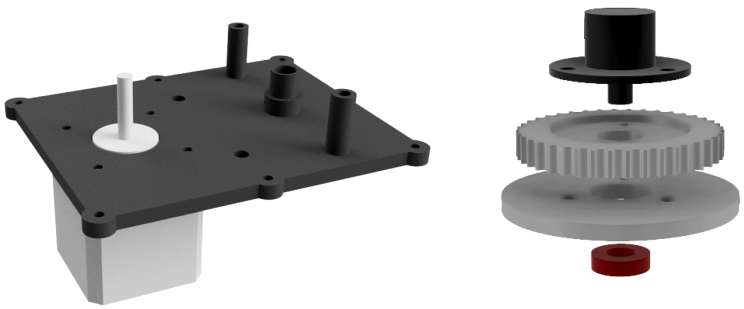

(a) Base

(b) Bearing and slip ring construction

Figure 4.3: (a) Overview of the base (black) and stepper motor (grey). (b) Exploded view of the bearing and slip ring construction, from top to bottom: slip ring (black), gear part (grey), flange part (grey) and bearing (red).

Base

The base consists of a part that supports the bearing from below. This bearing support is located in line with the stepper motor axle, as can be seen in Figure 4.3a. The pillars on either side of the bearing support

are used to mount a magnet, which is used for the motor control of Motor B (discussed in Section 5.5). The base also has space to mount the stepper motor, which drives the rotating part with a belt, and a hole for a belt tensioner. The base is designed in such a way that a box, in which the stepper motor and its corresponding driver are placed, can be designed and mounted to the bottom of the base.

4.2.2 Building material

To fabricate all the parts described above, a 3D printer is used, more specifically the Ultimaker 2+. The use of a 3D printer allows us to create custom parts quickly, with great accuracy and at an affordable price. The material used is Polylactic acid (PLA), this is a common type of 3D printing filament and it is strong enough for our purposes.

To design our parts we used Fusion 360 by Autodesk [Autodesk, 2019]. This software is free for students and is said to have a quicker learning curve compared to for example SolidWorks [Dassault Systmes SolidWorks Corp., 2018].

To prepare a design to be printed with an Ultimaker, the software programme Cura is used [Ult, 2019]. Cura slices the design into layers that can be printed using an Ultimaker. Cura has a lot of different settings that can be changed according to what needs to be printed. The choice was made to print everything with 100% infill, meaning there are no hollow parts in the components to save material. The reason everything is printed with 100% infill is the fact that most components are structural and a large part of the construction is rotating. Printing with 100% infill ensures the components are strong enough. Another setting that is used, is the "support" setting. This setting prints a separate support structure under overhanging parts of a design, like the countersunk holes for the bolts mentioned in Section 4.2.1. The layer height that is used on all of the 3D printed parts is $0.15\,\mathrm{mm}$.

4.3 Results and discussion of the construction

In this section we will discuss the results of the implemented construction and discuss to which extent the requirements are reached.

For the system requirement on the dimensions of the system, the 'Could have' requirement is reached. The construction can rotate withing a box of $0.24\,\mathrm{m} \times 0.24\,\mathrm{m} \times 0.2\,\mathrm{m}$. Further more, the light source can span an entire sphere, apart from the part that is obstructed by the construction itself. The construction obstructs the pattern in the shape of a cone beneath the origin of the light (the mirror) of roughly $90°$. The distance between the mirror and the light source can be adjusted to match the focal length. A slip ring is integrated into the construction to transfer power to the rotating part of the design. All the parts of the construction are 3D printed with PLA and are strong enough to withstand the stress during operation. Thus all the requirements for the construction are met.

Chapter 5: Motors

The construction consists of two motors which drive the rotation of the system. First, we will elaborate on the theory of electric motors and on PID motor control in Section 5.1 and Section 5.2 respectively. Then we will discuss the projection method in Section 5.3. After that, we will discuss Motor M and Motor B in detail in respectively Section 5.4 and Section 5.5.

5.1 Electric motor theory

In this section we will discuss the different types of motors and briefly elaborate on their properties, with which we can make a well informed choice for Motor M and Motor B. Some commonly used terms regarding electric motors are defined below:
Stator: The 'stator' is the non-moving part of a motor. The stator is often on the outside of the the rotor.
Rotor: The 'rotor' is the moving part of the motor. The rotor is connected (directly for non-geared, indirectly for geared motors) to the axis of the motor.
AC/DC: AC stands for Alternating Current and DC stands for Direct Current. Both types of current can be used to deliver power to the motor. The type determines the topology of the motor.
Three-phase: Three-phase is a method for AC power transportation. Three out of phase currents/voltages are used to deliver power (instead of one).

Now we will discuss different types of motors and elaborate on their properties.

AC motor An AC motor exploits the force between two rotating magnetic fields. The rotating magnetic field on the stator is created by three-phase AC currents. Because AC motors have no brushes that wear over time, they are effectively maintenance free. However, the accurate speed/torque control of AC motors is rather complex and expensive [Kim, 2017, p.5-6,36].

Brushed DC motor In a DC motor there are two stationary magnetic fields. The magnetic field in the rotor is kept stationary by the use of brushes and commutators. They make sure the current distribution in the rotor windings is always the same, even when the rotor is spinning. The main advantage of DC motors is their simple speed and torque control. This is the result of the fact that the speed is directly proportional to the applied voltage and the torque is directly proportional to the current. One disadvantage of a DC motor is the fact that the brushes wear out over time and thus require maintenance to ensure reliability [Kim, 2017, p.5,36].

Brushless DC motor Brushless DC motors (BLDC) were developed to get similar electrical characteristics as a brushed DC motor, but without the mechanical commutation. BLDCs use electronic commutation by placing the armature windings on the stator side and the magnets on the rotor side. The control of a BLDC motor is somewhat similar to the control of an AC motor but (semi) square waves are used instead of sine waves . The control of a BLDC motor is a bit more complex than that of a brushed DC motor, but BLDC motors are more reliable. The cost of BLDC motors is usually higher than brushed DC motors [Kim, 2017, p.389-391].

Stepper motor A stepper motor is a brushless DC motor, thus with permanent magnets on its rotor and electromagnets on its stator. The magnetic fields of the electromagnets are controlled in such a way that the permanent magnets on the rotor are pushed/pulled to the next 'step'. A stepper motor can thus only be in a limited amount of positions, called steps. This is different than a 'normal' brushless DC motor that is designed to have a smooth rotation. A stepper motor is often rated at a certain amount of degrees per step, which determines the amount of positions ($= \frac{360^\circ}{^\circ/\text{step}}$) per rotation. Due to these steps, a stepper motor is able to rotate to an exact amount of degrees or to rotate with a constant amount of steps per time unit. In addition to this, stepper motors usually have a high torque rating. The control of a stepper motor is slightly more complicated than the control of a 'normal' DC motor because of the specific order in which the electromagnets are controlled.

At low speeds a stepper motor can become less smooth, because vibrations are introduced after every taken step. This can be seen as a disadvantage. A solution to this problem is called microstepping. One step is divided into smaller so called microsteps. This is done by controlling the electromagnets on the stator with a PWM signal, instead of a DC value. Microstepping divides one rotation in more steps, thereby smoothing out the motion. However, the smooth rotation comes at a cost, because the torque per step decreases. The microsteps may not be as accurate as the normal steps, especially when a load is connected to the shaft of the motor. In addition, the control of a stepper motor becomes more difficult when microstepping is introduced.

5.2 PID control theory

In this section we will discuss a commonly used control mechanism; the proportional-integral-derivative control (PID control). Such a control mechanism can be used in a system, with a motor and a form of feedback, to control the motor speed.

A PID controller stabilises its output value by comparing the output with the desired value, the setpoint, and adjusting the output accordingly. To calculate the adjustment the error is defined as the difference between the output value and the setpoint. The mechanism calculates the adjustment using Equation 5.1, which consists of three factors, namely the proportional factor (k_P), the integral factor (k_I) and the derivative factor (k_D). These three factors are multiplied with the instantaneous error, the integral of the error over time and the derivative of the error over time respectively.

The proportional term reduces the steady-state error, but can not remove it. Further more it decreases the damping of the system. The addition of an integral term can be used to further reduce the steady-state error. Contrary to the proportional term, the integral term can, in theory, reduce the steady-state error to zero. The integral term also decreases the settling time of the step response of the system. Finally a derivative term can be used to speed up the system. It decreases the settling time and reduces overshoot [Franklin et al., 2015, p.196-203].

$$A(e) = k_P \cdot e + k_I \cdot \int e \cdot dt + k_D \cdot \frac{\partial e}{\partial t} \tag{5.1}$$

5.3 Projection method

In this section we will give a description of the projection method, to help understand the dependency between Motor M and Motor B.

There are multiple ways to span a sphere with two axes of rotation. In combination with the subgroup that focused on the control of the system, we chose a projection method, which will we will describe here. Motor M will spin faster than Motor B, in such a manner that Motor B makes a step every time Motor M has finished a complete rotation. For this reason Motor B will be implemented with a stepper motor. Half a rotation of Motor B will account for one projection. With this implementation, the frequency of Motor M should be a multiple of the frequency of Motor B to ensure the starting point and the endpoint of a projection coincide.

From simulations, done by the controller subgroup, it was concluded that in order to achieve enough accuracy in the projection, the step size of Motor B should be smaller than the required angular resolution.

The opening angle of the light source is adjusted to be equal to the angular resolution. Therefore a smaller step size will create overlap in the illumination between rotations of Motor M. Running these simulations with the step size of Motor B being four times smaller than the angular resolution gave satisfactory results.

5.4 Motor M

In this section we begin with the requirements for Motor M, followed by the implementation and the results and discussion of this implementation.

5.4.1 Requirements for Motor M

In this section we discuss the requirements on speed, steady-state error of the speed, speed deviation, start-up time and power consumption for Motor M.

Speed The speed of Motor M, in combination with the speed of Motor B, influences the angular resolution in longitudinal direction and the projection time of the system, which are both part of the system requirements, defined in Chapter 3.
To meet the system requirements that are set for angular resolution, Motor M needs to spin a specific amount of times faster than Motor B. The amount of times Motor M needs to spin faster than Motor B can be calculated by Equation 5.2, in which the factor 4 accounts for the desired illumination overlap described in Section 5.3.

$$\frac{f_{\text{Motor M}}}{f_{\text{Motor B}}} = \frac{180^\circ \cdot 4}{\text{Angular resolution } (^\circ)} \tag{5.2}$$

To meet the system requirements that are set for the projection time, Motor M should rotate at a minimum speed. The speed that Motor M needs to rotate at, in order to reach a specific projection time can be calculated using the following equation:

$$f_{\text{Motor M}} = \frac{180^\circ \cdot 4}{T_{\text{Projection}} \cdot \text{Angular resolution } (^\circ)} \tag{5.3}$$

The required speeds for Motor M for different combinations of angular resolution and projection time are stated in Table 5.1. These speeds are calculated using Equation 5.3 (with $T_{\text{projection}}$ in minutes).

Table 5.1: Required Motor M frequency in order to reach specific system requirements.

Projection time\Angular resolution	15°	5°	$< 5^\circ$
15 min	$3.2\,\text{rev min}^{-1}$	$9.6\,\text{rev min}^{-1}$	$> 9.6\,\text{rev min}^{-1}$
1 min	$48\,\text{rev min}^{-1}$	$144\,\text{rev min}^{-1}$	$> 144\,\text{rev min}^{-1}$
1 s	$2880\,\text{rev min}^{-1}$	$8640\,\text{rev min}^{-1}$	$> 8640\,\text{rev min}^{-1}$

Steady-state error of the speed The steady state error of the motor speed is the difference between the stable speed the motor reaches and the setpoint of the motor speed. The requirements on this parameter are based on the system requirements on phase drift, more specifically in latitudinal direction, stated in Table 3.1. The phase drift requirements are given in degrees. These requirements are converted from degrees to percentages by multiplying the degrees by $\frac{100\,\%}{360^\circ}$. These percentages represent the allowed steady-state speed error and are shown in Table 5.2.

Speed deviation Speed deviation is the deviation in speed, with respect to the average speed, once the motor has reached a stable frequency. The requirement on maximum speed deviation is defined by the system requirement on maximum phase error, more specifically in latitudinal direction, which is stated in Table 3.1. For the requirement for the speed deviation of Motor M, stated in Table 5.3, the numbers from the system requirements are converted from degrees to percentages by multiplying the degrees by $\frac{100\,\%}{360^\circ}$.

Table 5.2: Maximum steady-state speed error allowed in order to meet the system requirement on phase drift.

Type	Must have	Should have	Could have
Phase drift	$7.5°$	$2.5°$	$< 2.5°$
Maximum percentage of steady-state error	$2.08\,\%$	$0.69\,\%$	$< 0.69\,\%$

Table 5.3: Maximum percentage of speed deviation allowed, in order to meet the phase drift requirement in colatitudinal direction.

Type	Must have	Should have	Could have
Angular resolution	$15°$	$5°$	$< 5°$
Maximum speed deviation	$4.17\,\%$	$1.39\,\%$	$< 1.39\,\%$

Start-up time The start-up time of Motor M is the time it takes for Motor M to reach its steady state. After the start-up time, the maximum speed deviations should be less than $1\,\%$. This requirement is defined by the system requirement on the start-up time, stated in Chapter 3. The requirements on the start-up time for Motor M are stated in Table 5.4.

Table 5.4: Requirements on the start-up time for Motor M

Type	Must have	Should have	Could have
Start-up time	$< 15\,\mathrm{min}$	$< 1\,\mathrm{min}$	$< 10\,\mathrm{s}$

Power consumption Finally there is a requirement on power consumption. This requirement equals the output of the mains ($230\,\mathrm{V} \cdot 16\,\mathrm{A}$). Although this requirement is for the entire system, it is expected that Motor M will consume around 30% of the total power of the system.

To get an indication of the maximum power this motor could use, when the whole system is battery powered, we looked at the typical power ratings of mobile phone charging batteries. These batteries are readily available and can usually deliver around $50\,\mathrm{W\,h}$[1]. This means Motor M could consume $50\,\mathrm{W\,h} \cdot 30\,\% = 15\,\mathrm{W\,h}$. In other words Motor M could run for one hour at $15\,\mathrm{W}$, which is more than enough time to finish a series of measurements. An overview of the requirements concerning power can be found in Table 5.5.

Table 5.5: Requirements on the power for Motor M

Type	Must have	Should have	Could have
Power	$< 230\,\mathrm{V}$, $16\,\mathrm{A}$ (mains)	-	$15\,\mathrm{W}$

5.4.2 Implementation of Motor M

In this section we will elaborate on the implementation of Motor M. First the choice concerning the type of motor will be discussed, then a description of the corresponding motor driver and the motor control will follow.

[1] The "Anker PowerCore $10\,000\,\mathrm{mA\,h}$" was used as a benchmark.

Choice of the motor type

For Motor M, a brushed DC motor was chosen, due to its simple speed and torque control. The wear of the brushes within the motor should not pose any problems, because it will not be operating for large amounts of time continuously. A brushless DC motor would probably last longer, but this does not result in an overall advantage, because the price of a brushless motor is usually higher than that of a brushed motor.

The chosen motor is an 'RS PRO DC motor' of $19.68\,\mathrm{W}$ and is rated at $19\,000\,\mathrm{rev\,min^{-1}}$, $3.3{-}7.2\,\mathrm{V}$, $4.41\,\mathrm{A}$ (at maximum efficiency) [MFA]. The specifications of this motor meet the requirements for Motor M. This is validated with measurements, discussed in Section 5.4.3.

Motor driver

In order to drive the motor at the desired speed, a PWM signal of $1.4\,\mathrm{kHz}$, coming from the microcontroller (STM32F401RE) is used. Although the DC motor should, in theory, be controlled with a constant DC voltage, the motor has no problems with a PWM signal, as long as the modulation frequency of the signal is high enough. It was found that a PWM frequency of $1.4\,\mathrm{kHz}$ was sufficient. By changing the duty cycle of the PWM, the average voltage will change and thus the speed of the motor will change. However, the microcontroller generates a PWM signal with an amplitude of $3.3\,\mathrm{V}$, but the RS PRO DC motor is rated at $7.2\,\mathrm{V}$ (max). For this reason a motor driver is needed, that converts a $3.3\,\mathrm{V}$ PWM signal into a $7.2\,\mathrm{V}$ PWM signal.

Topology of the motor driver The circuit of the motor driver that is designed for this project, is shown in Figure 5.1. This circuit increases the amplitude of the PWM signal. It consists of two inverting transistor stages. When the PWM signal at the input is high, the NPN transistor is open, thereby pulling the gate of the PMOS transistor down (to ground). In this situation V_{GS} is negative and the PMOS transistor is conducting. Thus, when the input of the driver is high, at $3.3\,\mathrm{V}$, the output of the driver is also high, but at $7.2\,\mathrm{V}$. When the input PWM signal is low, the NPN transistor is closed and the gate of the PMOS transistor is pulled up (to $7.2\,\mathrm{V}$). In this situation the V_{GS} is (close to) $0\,\mathrm{V}$ and the PMOS transistor is not conducting. Thus when the input of the driver is low, $0\,\mathrm{V}$, the output of the driver is also low, $0\,\mathrm{V}$. To protect the motor driver from voltage spikes or any voltage ripple coming from the power supply, a decoupling capacitor is used.

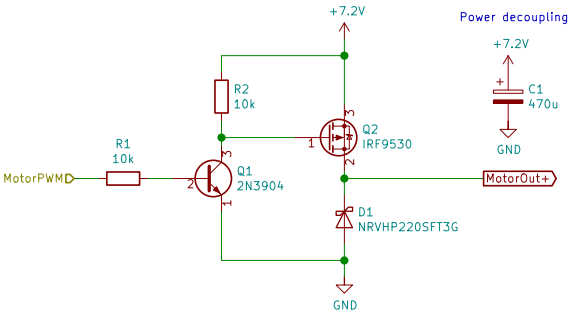

Figure 5.1: Motor drive circuit

Simulation of the motor driver The functionality of the motor drive circuit (Figure 5.1) was checked with a simulation in LTspice [Lin, 1999]. First, the circuit was simulated with a purely resistive load, this resulted in the operation that was expected; the circuit increases the amplitude of the input signal without changing any other parameters. Then the circuit was simulated with a resistor and inductor as load, which is a simple model for the DC motor. The resistor is taken $2\,\Omega$ and the inductor $87.7\,\mu\mathrm{H}$, to match the characteristics of the chosen motor. The input signal is a PWM signal with a duty cycle of $90\,\%$. The result of this simulation is shown in Figure 5.2. In this simulation the circuit also shows the right response; it increases the amplitude of the input signal. When the input is high ($3.3\,\mathrm{V}$), the output goes to $6.29\,\mathrm{V}$, instead of $7.2\,\mathrm{V}$, and $3.14\,\mathrm{A}$. This voltage difference is due to the voltage drop over the PMOS transistor. The voltage drop will result in a small decrease of maximum speed of the motor, which is not a problem since the motor will never operate on its maximum speed, $19\,000\,\mathrm{rev\,s^{-1}}$.

To determine the right component values, results of the same simulation were used. The RMS current and the peak current flowing through all the components were measured. The results of this simulation can be found in Table 5.6.

Table 5.6: Overview of currents flowing through the components of the motor drive circuit (Figure 5.1), with a $90\,\%$ duty cycle PWM input signal

Component	RMS current (A)	Peak current (A)
R_1	1.61×10^{-4}	2.62×10^{-4}
R_2	5.98×10^{-4}	7.18×10^{-4}
Q_1	5.30×10^{-3}	1.95×10^{-2}
Q_2	2.19	3.14
D_1	5.93×10^{-1}	2.34

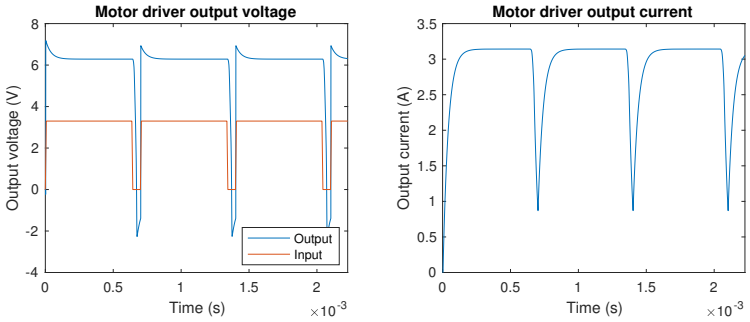

Figure 5.2: Motor driver output voltage and current, with a $90\,\%$ duty cycle PWM input signal.

Component choice of the motor driver The first stage could be implemented with different types of transistors, but a simple NPN transistor suffices. This is because only small currents, of maximally $19.5\,\mathrm{mA}$, will flow through the device. The second stage needs a transistor capable of conducting a lot of current, since this is the stage that drives the motor. The simulation shows a $2.19\,\mathrm{A}$ RMS and $3.14\,\mathrm{A}$ peak value. For this reason a P-channel power MOSFET is needed. The two resistors, R_1 and R_2, should have a value high enough to prevent high currents to flow through the NPN transistor. If a resistance of $10\,\mathrm{k\Omega}$ is used, an RMS current of only $0.161\,\mathrm{mA}$ and $0.598\,\mathrm{mA}$ will flow through respectively R_1 and R_2. A general NPN transistor should be able to handle currents in the order of mA. The diode is used as flyback diode to protect the motor driver from back EMF current coming from the motor, due to the inductive behaviour of the windings. Therefore, the diode should be able to handle high currents. The simulation shows an RMS current of $593\,\mathrm{mA}$ and a peak current of $2.34\,\mathrm{A}$.

All the components should handle the discussed voltages and currents. The exact components that were used for this project can be found in Figure 5.1.

Motor control

As already mentioned, the motor is controlled by a PWM signal coming from the microcontroller. The speed of the motor can be controlled with the duty cycle. However, when a PWM signal with a constant duty cycle is applied, the motor axis does not rotate with a constant speed, due to imperfections in the motor and due to influences from the environment. To ensure the speed stability of Motor M, a motor control system is required.

The motor control system is implemented with a single feedback loop. The motor speed is continuously measured using a Hall effect switch. A Hall effect switch is a device that switches its output from high to low if the magnetic flux density in the device reaches a certain threshold, and pulls it up if the magnetic flux density goes down again. By mounting a permanent magnet on the rotating axis and placing the Hall effect switch on the non-moving part (or the other way around - although this choice makes it more difficult) a block pulse signal is created. This signal has exactly the same frequency as the motor frequency. The signal is fed back to the microcontroller which measures the period length of the signal. In this way the microcontroller can compensate for any frequency errors by adjusting the duty cycle of the PWM signal to the motor. The microcontroller uses a PID controller to calculate the right adjustment. To calculate the

PID constants, the parameters of Motor M need to be identified. These parameters were estimated using the method proposed by Wu [2012]. The parameter estimation method and other calculations that were used to find the PID constants, which result in a desired response, are given in Appendix B. The resulting PID values are $k_P = -7.672\,\mathrm{s\,rad^{-1}}$, $k_I = -1.4796 \times 10^{-5}\,\mathrm{rad}$ and $k_D = -4.217 \times 10^{-2}\,\mathrm{s^2\,rad^{-1}}$. A schematic overview of the implemented control system for Motor M can be seen in Figure 5.3.

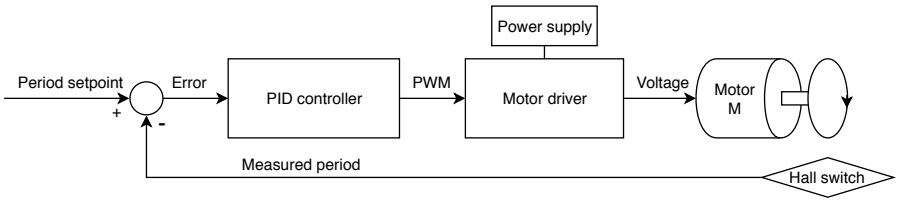

Figure 5.3: Schematic overview of the control system for Motor M.

In addition to the speed adjustments from the PID controller, the microcontroller resets the projected pattern each time the Hall effect switch pulls its output down. In this way the pattern is reset at the start of each rotation and large fluctuations in the speed of Motor M, spread out over multiple rotations, do not influence the pattern. Figure 5.4 shows the circuit with the Hall effect switch. Node 2 is the output signal of the device. R_{hall} is used as pull up resistance, which limits the output current. The Hall effect switch is only capable of driving its output with $I_{out,max} = 25\,\mathrm{mA}$. Thus Equation 5.4 must hold and R_{hall} must be larger than $132\,\Omega$ [All]. The exact components that were used for the circuit can be found in Figure 5.4. The magnet that was used, is made of neodymium.

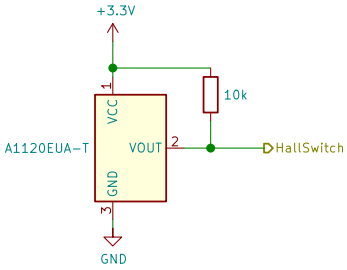

Figure 5.4: Hall effect switch circuit

$$\frac{V_{cc}}{R_{hall}} < I_{out,max} \tag{5.4}$$

5.4.3 Results and discussion of Motor M

This section will first elaborate on the results of the implementation, then the results will be compared with the requirements for Motor M.

Results of Motor M

In this section we discuss the results of the implementation of the motor driver and the motor control.

Motor driver Measurements with varying duty cycles were performed in order to test the functionality of the motor driver for Motor M. Figure 5.5 shows the output waveform of both the simulation and the actual motor driver, both with a 70% duty cycle input PWM signal. It can be seen that these waveforms differ. This is mainly due to the fact that the DC motor was modelled as a series connection of a resistor and an inductor. Although such a model includes the inductive behaviour of the motor, other aspects such as the actual movement of the motor are not taken into account. Figure 5.5 shows the RMS voltage of the motor drive circuit and simulation corresponding to different duty cycles. It can be seen that both curves are not linear. This is due to the non-idealities of a DC motor. However, the motor driver output is a one to one function of the duty cycle and the motor will be controlled using a feedback loop. For this reason the non-linearity of the motor driver does not form a problem.

Motor control Figure 5.6 shows the step response of the control system for Motor M, that is depicted in Figure 5.3. During the measurement for this step response, the mirror mount was connected to Motor M as a load. The characteristics of the step response are stated in Table 5.7.

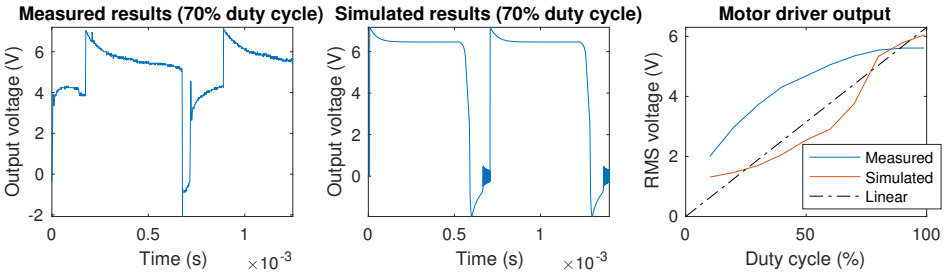

Figure 5.5: *Left and middle:* Measured and simulated motor driver output voltage, with a 70 % duty cycle PWM input signal. *Right:* Measured and simulated motor driver RMS output voltage, with duty cycles ranging from 10 % to 99 %.

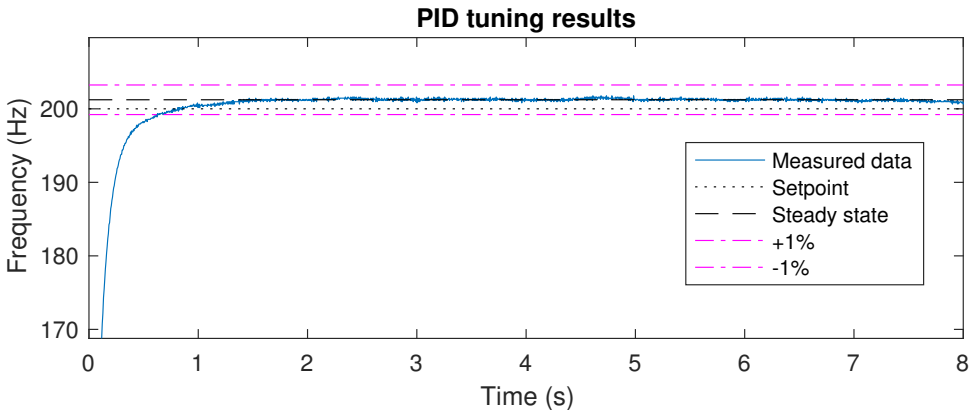

Figure 5.6: Step response of the system with PID control. PID constants: $k_P = -7.672$, $k_I = 1.477 \times 10^{-5}$, $k_D = 4.217 \times 10^{-2}$

Discussion of Motor M

Driving Motor M with a 90 % duty cycle resulted in speeds up to 20 400 $\mathrm{rev\,min^{-1}}$, which is enough to meet the 'Could have' system requirements for both projection time and angular resolution, as long as Motor B can also meet the requirements for the 'Could have' category.

The steady-state error of the motor speed is 0.62 %, which is within the 'Could have' requirement on steady-state error (steady-state error < 0.69 %). Although there is a steady-state error, this error does not contribute to the phase drift of the system, because of the synchronisation with the Hall effect switch.

The maximum speed deviation of Motor M is 0.29 %. Thus the 'Could have' requirement on the speed deviation of Motor M (Speed deviation < 1.39 %) is reached.

The system takes 0.68 s to achieve a stable output between ± 1 % of the steady-state. This settling time contributes to the start-up time of the system, which is a system requirement, stated in Chapter 3. The requirement is still within the 'Could have' category, but this also depends on the start-up time of the other subsystems.

Concerning power consumption, 'Must have' requirement has been reached. At 90 % duty cycle, the

Table 5.7: Step response characteristics

Characteristic	value
Settling time (± 1 %)	0.68 s
Steady-state error	0.62 %
Max. speed deviation	0.29 %

output of the motor driver has values up to $6.29\,\mathrm{V}$, $3.14\,\mathrm{A}$. Thus Motor M uses up to $19.8\,\mathrm{W}$, at $90\,\%$ duty cycle. This would probably not be practical to draw from a reasonably sized battery.

5.5 Motor B

This section begins with the requirements for Motor B, then the implementation and the results and discussion of the implementation follow.

5.5.1 Requirements for Motor B

In this section the requirements on speed, speed deviation and power consumption for Motor B are discussed.

Step frequency and step size The speed of Motor B, in combination with the speed of Motor M, influences the angular resolution in longitudinal direction and the projection time of the system, which are both part of the system requirements, defined in Chapter 3.
As Motor B will be implemented with a stepper motor, the step size also influences the angular resolution and projection time. The most common step size of a stepper motor is $1.8°$. With a $1.8°$ step size, it takes 200 steps to complete half a rotation and thus one full projection. Furthermore a higher angular resolution can be reached by using the microstepping technique. An overview of the required step frequencies, for different step sizes and projection times, can be found in Table 5.8. These step frequencies are calculated using the following equation (with $T_{\text{projection}}$ in seconds):

$$f_{\text{step}} = \frac{180°}{\text{Step size}(°) \cdot T_{\text{Projection}}} \tag{5.5}$$

Table 5.8: Required Motor B step frequency (Hz) in order to reach the system requirements on projection times, for different step sizes

Projection time\Step size	$1.8°$	$0.9°$	$0.45°$
$15\,\mathrm{min}$	$1.11 \times 10^{-1}\,\mathrm{Hz}$	$2.22 \times 10^{-1}\,\mathrm{Hz}$	$4.44 \times 10^{-1}\,\mathrm{Hz}$
$1\,\mathrm{min}$	$1.67\,\mathrm{Hz}$	$3.33\,\mathrm{Hz}$	$6.67\,\mathrm{Hz}$
$1\,\mathrm{s}$	$100\,\mathrm{Hz}$	$200\,\mathrm{Hz}$	$400\,\mathrm{Hz}$

Step inaccuracy The requirement on step inaccuracy is defined by the system requirements on maximum phase error, more specifically in longitudinal direction, which is stated in Chapter 3. When a step is missed, this contributes to the phase error. The percentages of allowable missed steps are given in Table 5.9.

Table 5.9: Maximum percentage of missed steps in order to reach the system requirements on maximum phase error, for different step sizes.

Maximum phase error\Step size	$1.8°$	$0.9°$	$0.45°$
$15°$	$8.33\,\%$	$4.17\,\%$	$2.08\,\%$
$5°$	$2.78\,\%$	$1.39\,\%$	$0.69\,\%$
$<5°$	$<2.78\,\%$	$<1.39\,\%$	$<0.69\,\%$

Power consumption Finally there is a requirement on power consumption. The reasoning behind this requirement is identical to the power requirement for Motor M. For this reason this will not be explained again. The power consumption requirements for Motor B are given in Table 5.10.

Table 5.10: Requirements on the power for Motor B

Type	Must have	Should have	Could have
Power	$< 230\,\mathrm{V}$, $16\,\mathrm{A}$ (mains)	-	$15\,\mathrm{W}$

5.5.2 Implementation of Motor B

This section elaborates on the implementation of Motor B. First the choice concerning the type of motor will be discussed, then a description of the corresponding motor driver and the motor control will follow.

Choice of the motor type

Motor B should be a stepper motor rated at a high resolution, or a low step size. The motor should be able to rotate the construction. The chosen motor is a NEMA17 Stepper motor [Chi] with $1.8°$ per step, which meets the requirements for Motor B.

Motor driver

Ideally the stepper motor is controlled by the microprocessor with a PWM signal, just like Motor B. However the stepper motor has four input wires that lead to the coils inside, thus a PWM signal can not directly be fed to the stepper motor. Therefore a motor driver is used. The motor driver makes sure that the motor takes one step each time it gets a pulse. The motor speed is determined by the frequency of such pulses, and not the duty cycle.

For this project the motor driver for the stepper motor was bought as a pre-assembled PCB [Rep]. This driver is able to perform microstepping, with step sizes down to $\frac{1}{32}$ of a full step, and drive its output with an output current of $2.5\,\mathrm{A}$. We chose to use half stepping, thus 400 steps ($0.9°$ each) per revolution instead of 200 per revolution. This resulted in a much smoother rotation, which reduces projection errors caused by vibrations of the system. Although microstepping reduces the torque per step, the motor still has enough torque to drive the construction.

To connect the stepper driver, the explanation in the datasheet [Rep] was followed. A $24\,\mathrm{V}$ power source is used to drive motor and a $5\,\mathrm{V}$ power source is used as logic voltage. By connecting this logic voltage to specific pins on the driver, it is possible to permanently enable the driver and select the half step setting that is needed.

Motor control

As mentioned before, the stepper motor is controlled by the frequency of the pulse signal, coming from the microcontroller. For this motor, a control mechanism is not needed, since the stepper motor takes exactly 200 steps per revolution. However, since half stepping is used, the step accuracy decreases and the motor skips a few steps sometimes. Measurements on this accuracy are discussed in the following section. As discussed in Chapter 4, two magnets are placed upon the base. Another Hall effect switch is placed upon the moving part of the construction. By doing this the microcontroller can synchronise the projection in such a way that a pattern always starts with the construction oriented in the same position.

5.5.3 Results and discussion of Motor B

This section will first elaborate on the results of the implementation of Motor B, then the results will be compared with the requirements for Motor B.

Results of Motor B

Since it was chosen to use microstepping (half stepping in this case), Motor B loses accuracy and the motor misses steps under certain conditions. Measurements were performed in order to test the accuracy of the motor under these different conditions. A function generator was used to give the motor driver 4000

pulses, thus 10 rotations while half stepping, each measurement. After these rotations the motor should stop at exactly the same place it started the measurement. The number of missed steps was counted. The measurements were performed for different step frequencies and different drive voltages. When rotating the construction with a typical step frequency of $200\,\mathrm{Hz}$, the power needed to drive the stepper motor is $24\,\mathrm{V} \cdot 0.7\,\mathrm{A} = 16.8\,\mathrm{W}$. The results of these measurements can be found in Figure 5.7.

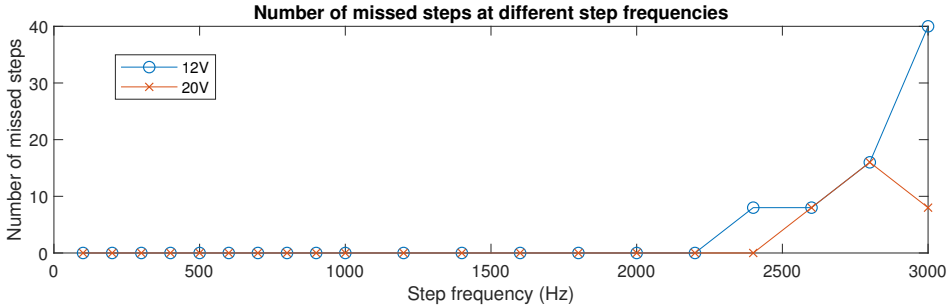

Figure 5.7: Number of missed steps, per 4000 steps, at different step frequencies and different drive voltages

The motor operates flawless at step frequencies up to $2.2\,\mathrm{kHz}$. At higher frequencies the motor starts missing steps, about $0.2\,\%$ to $1\,\%$ of the total steps. By increasing the drive voltage, the average number of missed steps is decreased. Since the torque of the motor also increases with an increasing drive voltage, it is desired to have a high drive voltage. For this project the stepper motor will operate at step frequencies below $\frac{19\,000\,\mathrm{rev\,min^{-1}}}{60\,\mathrm{s\,min^{-1}}} \approx 317\,\mathrm{Hz}$, because the step frequency has to be equal to the frequency of Motor M. In this step frequency range the stepper motor works as desired.

Discussion of Motor B

Motor B is able to rotate the construction with a step frequency up to $2.2\,\mathrm{kHz}$ and steps of $0.9°$, using half stepping. With these results Motor B can meet the ”Could have” requirement on projection time.

Operating at this step frequency and step size, the percentage of missed steps is $< 1.39\,\%$. Therefore Motor B is also able to meet the ’Could have’ requirement on maximum phase error ($< 5°$).

Motor M and Motor B are both able to reach the ’Could have’ category of the system requirements on projection time and maximum phase error. Therefore the combination combination of the two is also able to reach the these system requirements.

Concerning the power consumption, the ’Must have’ requirement has been reached. During typical operation, the stepper motor uses roughly $16.8\,\mathrm{W}$. With this power rating it will not be practical to deliver the power with a readily available battery, since the estimated power budget when using such a battery is $15\,\mathrm{W}$.

Chapter 6: Power distribution

To deliver power to all the subsystems at the right ratings, a power supply was designed. This chapter describes the power supply in detail. First some theory on power converters is given in Section 6.1, then the requirements of the power supply and the implementation follow in Section 6.2 and Section 6.3. Finally the results of this implementation are discussed in Section 6.4.

6.1 Power converter theory

As will be explained in Section 6.3.2, we will not design our own AC/DC converter. For this reason we will only elaborate on DC/DC converter theory. In this section two different DC/DC converters will be discussed, namely a linear regulator and a switching regulator.

6.1.1 Linear regulator

The linear regulator is a straightforward step down converter. It makes use of the variable resistance behaviour of a transistor. The linear regulator uses a feedback loop to adjust the variable resistance in such a way that a constant output voltage is obtained. The voltage difference between the input and the output is dissipated into heat by the variable resistance, which is the main disadvantage of a linear regulator. This type of DC/DC converter can only be used as a step-down converter. The converter needs a certain voltage drop in order to work, this is called the drop-out voltage.

6.1.2 Switching regulator (Buck converter)

The switching regulator has several applications, namely as buck converter, as boost converter and as buck-boost converter. The different applications are used to respectively step up, step down and either step up or down the voltage. Here only the buck converter will be discussed, because it is a step down converter. Motivation on the use of step down converters can be found in Section 6.3.1.

The step-down switching regulator switches its output by pulling it up, to the input voltage, or down, to ground. An energy storage unit, connected to the output of the switching regulator, is used to store energy if the output of the switching regulator is high and to deliver energy to the load if the output of the switching regulator is low. In most cases an inductor, cascaded in series with the output of the switching regulator, is used as energy storage unit. A switching regulator is a more advanced converter, when compared to the linear regulator, but it is more efficient, especially when a large step down voltage is required.

6.2 Requirements for the power supply

The voltage and current ratings that the different subsystems require to operate, define the requirements for the power supply. The identified requirements are listed in Table 6.1 and the power ratings of the subsystems are listed in Table 6.2. The requirement for the power source is taken from Chapter 3. The requirement for the output only has a 'must have' because it is essential for the system, but can not be further improved once it works and therefore has no 'should have' or 'could have'.

Table 6.1: The requirements for the power supply

Type	Must have	Should have	Could have
Power source	The mains, 230 V, 16 A	-	battery powered
Output	The power supply delivers power to the different components of the system at the ratings, listed in Table 6.2.	-	-

Table 6.2: The required voltage and current ratings of the different subsystems

Subsystem	Voltage (V)	Max. current (A)
Motor M	7.2	3.5
Motor B	24	1
Driver for Motor B	5	250×10^{-6}
Microcontroller	3.3	0.2
Light source	12	0.1

6.3 Implementation of the power supply

In this section the implementation of the power supply is presented. First the topology of the power supply is given, then the subsystems of the power supply are discussed individually.

6.3.1 Topology of the power supply

The power supply is designed to operate connected to the mains. This coincides with the 'must have' requirement for power. This implementation is cheaper and quicker than an implementation using a battery.

The power supply is implemented with two AC/DC converters and three DC/DC converters of which one is a switching regulator and the other two are linear regulators. All of these converters are step down converters, because all of the voltages that are needed in the system are lower than the 230 V coming from the mains. Although the power supply is shown as one whole in Figure 6.1, it actually consists of two parts which are connected via a slip ring; the stationary part and the rotating part. The implementation of the five converters and the slip ring will be discussed in detail in the following sections.

6.3.2 Subsystems of the power supply

In this section the subsystems of the power supply are discussed individually.

AC/DC converter (12 V)

An AC/DC converter, positioned on the stationary part, is needed to convert 230 VAC (mains) to 12 VDC, to be fed to the rotating part of the system. The lab, where the system was built and tested, has various safety rules, which do not allow to build systems that are supposed to operate at voltages above 45 V. For this reason an AC/DC converter was bought. For this project a converter rated at 12 V, 4 A was used [XP , b].

AC/DC converter (24 V)

Another AC/DC converter, positioned on the stationary part, is needed to convert 230 VAC (mains) to 24 VDC, to supply Motor B. This AC/DC converter was bought, for the same reasons as the previous AC/DC converter. For this project a converter rated at 24 V, 1 A was used [XP , a].

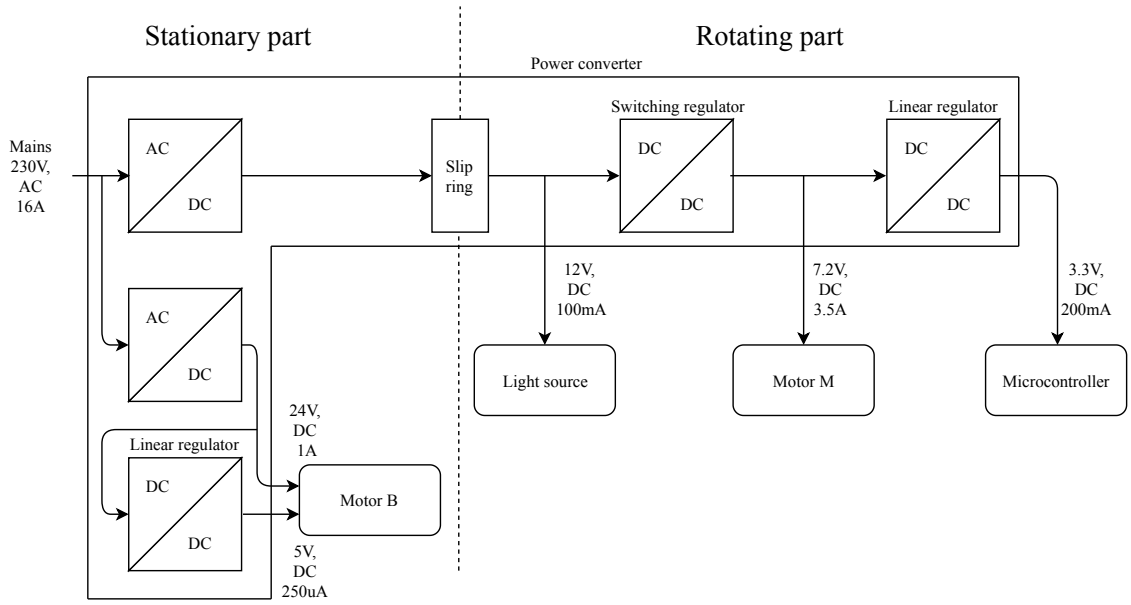

Figure 6.1: Block diagram of the implemented power supply

5 V converter

This DC/DC converter, positioned on the stationary part, converts the 24 V into 5 V. It is used for logic voltages to make the driver for Motor B operate correctly. This section discusses the implementation of this converter. First the choice of regulator type is explained, then the corresponding circuit topology is discussed.

Choice of regulator type The converter is used to supply logic voltages that do not require large currents. The motor driver for Motor B, the DRV8852 [Rep], has a pull down resistance of 100 kΩ, which corresponds with 50 µA per logic port. Since the driver has five logic ports, this corresponds with 250 µA. At these power ratings, heat dissipation, will not be a problem. Therefore this converter does not need the high efficiency of a switching regulator to prevent heat dissipation and a linear regulator will suffice. In addition, a linear regulator is simple to implement and takes up less space than a switching regulator. For this reason, an implementation with a linear regulator is the best choice.

For this project, a UA7805 [Tex, b] is used as linear regulator. It has an input voltage range from 5.3 V to 25 V and can deliver an output current up to 1.5 A, which is more than enough for this application.

Topology of the converter circuit An overview of the circuit is shown in Figure 6.2. The linear regulator only needs an input and output capacitor to reduce the voltage ripple at the input and at the load respectively. The values for these capacitors are taken from the typical values given in the datasheet of the device [Tex, b] and are stated in Figure 6.2.

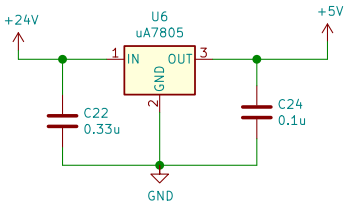

Figure 6.2: 5.0 V converter circuit

Slip ring

In order to get power from the stationary part to the rotating part, a slip ring or a wireless connection can be used. An implementation with a slip ring is a lot faster than a wireless implementation. This is mainly due to the fact that there is no need for a protocol when transferring low frequency signals over a slip ring. When using a wireless protocol, this protocol needs to be encoded and decoded, which is time consuming.

For this project a slip ring with six wires was used [Ada]. The wires are rated 240 V, 2 A each. The operating speed is rated at 300 $\mathrm{rev\,min^{-1}}$. To test the performance of the slip ring when it is rotating,

a measurement was performed. A brief description and the results of this measurement can be found in Appendix D. The conclusion of this measurement is that the slip ring functions well, even when rotated at higher speeds than $300\,\mathrm{rev\,min^{-1}}$.

7.2 V converter

This DC/DC converter, positioned on the rotating part, converts the $12\,\mathrm{V}$ into $7.2\,\mathrm{V}$. It delivers the power to Motor M and to the second DC/DC converter. This section discusses the implementation of this converter. First the choice of regulator type is explained, then the corresponding circuit topology is discussed.

Choice of regulator type The converter needs to be able to deliver current up to $3.5\,\mathrm{A}$, in order to drive Motor M properly. To prevent heat problems, a high efficiency is desired for this converter. For this reason, an implementation with a switching regulator is the best choice for this converter.

For this project, an LM2679 [Tex, 2016] is used as switching regulator. This device has a large input voltage range ($8\,\mathrm{V}$-$40\,\mathrm{V}$) and an adjustable output voltage range ($1.2\,\mathrm{V}$-$37\,\mathrm{V}$). The output voltage is adjusted with the values of the components around the integrated circuit (IC). It is able to deliver an output current up to $5\,\mathrm{A}$ and has a high efficiency, typically around $80\,\%$. Thus the device suffices for this application.

Topology of the converter circuit An overview of the circuit is shown in Figure 6.3. The inductor L_1 stores energy when the output of the switching regulator (U_7), called SwitchOutput, is high and delivers energy to the load when this output is low. The input and output capacitors (C_{21}, C_{23}, C_{27}) are used to reduce the voltage ripple at the input and at the load respectively. The diode is used as flyback diode to protect the switching regulator from the voltage spikes, generated by the inductor when the switching regulator is switching its output from high to low. The values and connection of the other components are specific to the chosen switching regulator, the LM2679. The values of these components were calculated using the datasheet of the device, and are stated in Figure 6.3. The calculations and motivation for all the component values can be found in Appendix E.

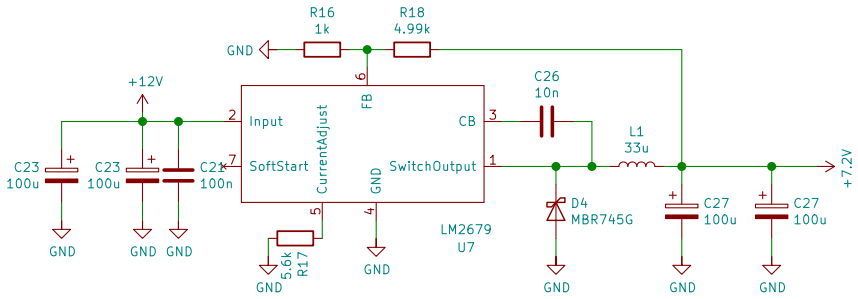

Figure 6.3: 7.2 V converter circuit

3.3 V converter

This DC/DC converter, positioned on the rotating part, converts the $7.2\,\mathrm{V}$ into $3.3\,\mathrm{V}$. It delivers power to the microcontroller. This section discusses the implementation of this converter. First the choice of regulator type is explained, then the corresponding circuit topology is discussed.

Choice of regulator type The converter delivers power to the microcontroller, which maximally needs $200\,\mathrm{mA}$. At these power ratings, heat due to dissipation, will not be a problem. Thus this converter does not need the high efficiency of a switching regulator to prevent heat dissipation and a linear regulator will suffice. In addition, a linear regulator is simple to implement and takes up less space than a switching regulator. For this reason, an implementation with a linear regulator is the best choice.

For this project, a UA78M33 [Tex, a] is used as linear regulator. It has an input voltage range from 5.3 V to 25 V and can deliver an output current up to 0.5 A, which is enough for this application.

Topology of the converter circuit An overview of the circuit is shown in Figure 6.4. The linear regulator only needs an input and output capacitor to reduce the voltage ripple at the input and at the load respectively. The values for these capacitors are taken from the typical values given in the datasheet of the device [Tex, a] and are stated in Figure 6.4.

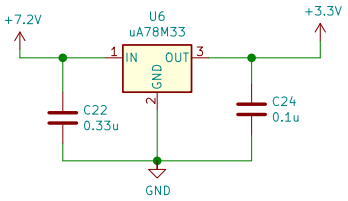

Figure 6.4: 3.3 V converter circuit

6.4 Results and discussion

In this section we will elaborate first on the results of the implementation of the power supply, then we will discuss to what extent the requirements for the power supply have been reached.

Results of the power supply

In this section the results of the implementation of the subsystems is discussed.

5.0 V converter The 5.0 V converter has a mean output voltage of 5.08 V and has maximum voltage deviation of 5.51 %. A graph of the output voltage can be found in the middle of Figure 6.5.

7.2 V converter The 7.2 V converter has an output voltage of 7.22 V and has maximum voltage ripple of 3.89 %. The frequency of this ripple is 1.4 kHz, this is probably due to the PWM driving of Motor M. A graph of the output voltage can be found on the left side of Figure 6.5.

3.3 V converter The 3.3 V converter has an output voltage of 3.36 V and has maximum voltage ripple of 3.57 %. The frequency of this ripple is 1.4 kHz, this is probably due to the PWM driving of Motor M. A graph of the output voltage can be found on the right side of Figure 6.5.

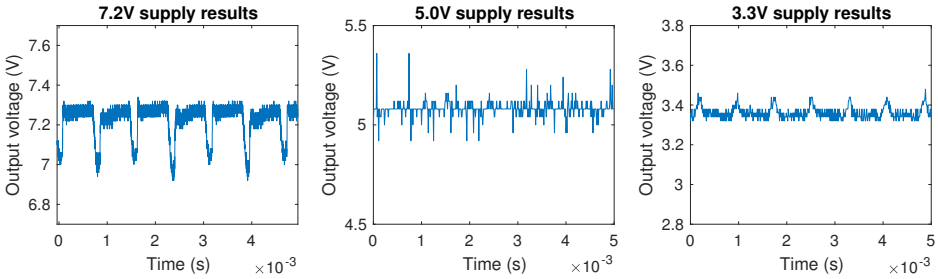

Figure 6.5: Output voltages of the DC/DC converters. *Left:*7.2 V supply, *Middle:*5.0 V supply, *Right:*3.3 V supply

Discussion of the power supply

All the converters deliver the desired output. Thus the power supply is able to deliver the power ratings that are required for the subsystems. For the requirement on power source, the 'Must have' category is reached. In order for the system to be battery powered, the power converter should be designed differently, since the battery typically has different ratings than the general power outlet (the mains).

Chapter 7: Prototype implementation and validation results

This section will discuss the last steps in the building of the measurement light bulb. First, the fabrication of the prototype will be discussed, followed by the test results of the complete system.

7.1 Fabrication of the prototype

The final prototype consists of all subsystems as shown in Figure 2.3. The subsystems, separately designed by the subgroups, are assembled together to form the prototype.

The laser, implemented in the final prototype, has an opening angle of $4°$ and is focused such that the focal point coincides with the mirror. By using this angular resolution, the spherical harmonic can be projected accurately while still limiting the time needed for each measurement. The construction has two axes over which it can rotate, which allows the laser to project onto a sphere around itself. The measurement light bulb acts as a point source, due to the fact the focal point coincides with the mirror, from which the spherical harmonic is projected into the room.

Motor M spins at $200\,\mathrm{Hz}$, while Motor B steps at $200\,\mathrm{Hz}$ with steps of $0.9°$, thus 400 steps for one rotation. This means that during the projection of one pattern, Motor B rotates $180°$, which corresponds with 200 steps. Therefore the projection of one pattern takes $1\,\mathrm{s}$. The microcontroller controls the speed of the two motors and synchronises this with the intensity of the laser to create a pattern. The synchronisation with the camera is not yet implemented, so the camera is controlled and set up manually.

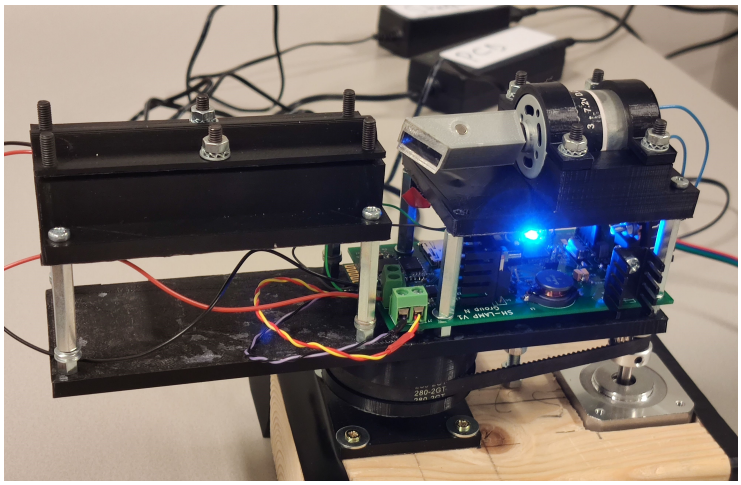

Figure 7.1: A photograph of the prototype

7.2 Results of complete system tests

The goal of this project was to build a measurement light bulb which can project spherical harmonics and to synchronise it with a camera so that the impact of the illumination can be captured. Figure 7.3 shows the result of a projection of the measurement light bulb. The photograph is taken in a dark environment to eliminate as much ambient light as possible, which is required since the laser is relatively low power. The exposure time for this photograph was 8 s. The pattern that is projected is the positive part of the spherical harmonic function of order 2 and index -2, of which a plot is depicted in Figure 7.2.

However, it still contains some errors. The positioning of the Hall effect switch for Motor M causes some offset in latitudinal direction, which should be corrected for. Also, a bug in the projection algorithm causes the spherical harmonic to be projected in two different orientations: once normally, and once rotated 180° over the longitudinal axis. These two errors combined make it that the projection is actually two projections of the same spherical harmonic oriented in slightly different ways.

Also, since the Hall effect switch for Motor B is not yet placed, the measurement light bulb is not yet able to orient itself longitudinally.

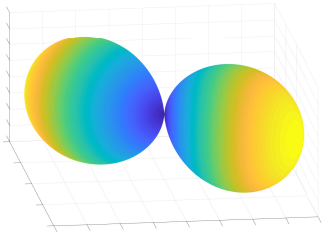

Figure 7.2: Plot of the positive part of the spherical harmonic function of order 2, index -2

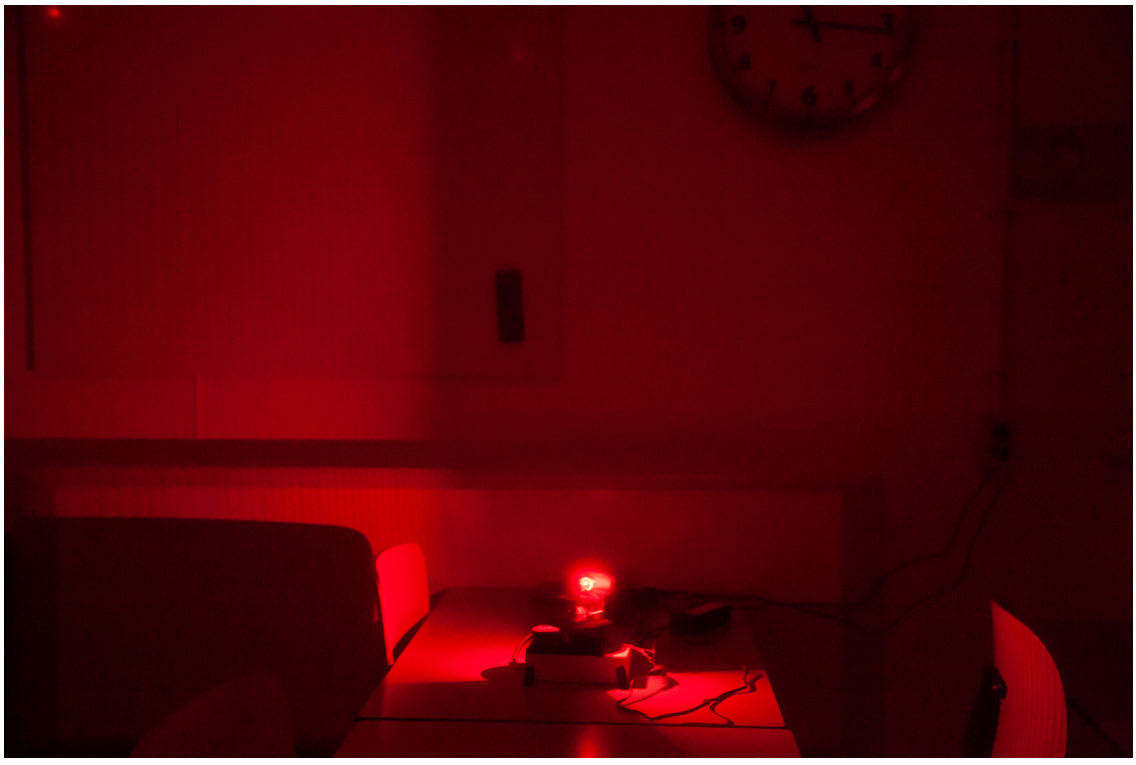

Figure 7.3: A photograph of the first spherical harmonics projection

Chapter 8: Discussion of results

In this section the results of the measurement light bulb are compared with the system requirements, stated in Chapter 3. Table 8.1 shows an overview of the system requirements and the results that are achieved.

Table 8.1: Overview of complete system requirements

Type	Must have	Should have	Could have	Result
Angular resolution	$15°$	$5°$	$<5°$	$4°$
Projection time	"converges"	$1\,\mathrm{min\,pattern^{-1}}$	$1\,\mathrm{s\,pattern^{-1}}$	$1\,\mathrm{s\,pattern^{-1}}$
Power	230 V, 16 A	-	battery powered	230 V, 16 A
Start-up time	$<15\,\mathrm{min}$	$<1\,\mathrm{min}$	$<10\,\mathrm{s}$	$1\,\mathrm{min}$
Dimensions	$1\,\mathrm{m}\times1\,\mathrm{m}\times1\,\mathrm{m}$	"fits through door" $<0.8\,\mathrm{m}$ for smallest rib	$0.4\,\mathrm{m}\times0.4\,\mathrm{m}\times0.4\,\mathrm{m}$	$0.24\,\mathrm{m}\times0.24\,\mathrm{m}\times0.20\,\mathrm{m}$
Phase drift	$7.5\,°\,\mathrm{rev^{-1}}$	$2.5\,°\,\mathrm{rev^{-1}}$	$<2.5\,°\,\mathrm{rev^{-1}}$	$0\,°\,\mathrm{rev^{-1}}$
Maximum phase error	$5°$	$5°$	$<5°$	$1.044°$
Colour of the light source	monochrome	-	RGBW	monochrome
SH order	0-1-2	-	higher orders	None
Brightness	Capturable in completely dark room	-	Visible in daylight	Capturable in completely dark room
Light levels	8 (3 bit)	256 (8 bit)	16384 (14 bit)	256 (8 bit)
Camera synchronisation	Change settings and take pictures manually	Change settings manually, use microcontroller to take pictures	Everything done by microcontroller	Change settings and take pictures manually
User interface	working UI	-	GUI	working UI

Angular resolution The final angular resolution of the system is equal to $4°$ and therefore the 'Could have' requirement is reached.

Projection time Since Motor B has a frequency of $0.5\,\mathrm{Hz}$ and one projection only needs a $180°$ rotation, the projection of one pattern takes $1\,\mathrm{s}$. Thus the and therefore the 'Could have' requirement is reached.

Power The system is powered using the mains. Therefore the 'Must have' requirement is reached. In order for the system to be powered by one or multiple batteries, the power supply should be designed differently to be compatible with the battery instead of with the mains.

Start-up time The device can start a measurement within one minute of switching the device on. Therefore the 'Should have' requirement is fulfilled. A faster start-up time would require a faster data transmission when a pattern is uploaded to the device, since this is the bottle neck for the start-up time.

Dimensions The measurement light bulb has the dimensions $0.24\,\mathrm{m}\mathrm{x}0.24\,\mathrm{m}\mathrm{x}0.20\,\mathrm{m}$. Therefore the 'Could have' requirement is reached.

Phase drift The phase drift of the pattern is equal to zero, since the pattern is reset each time Motor M finishes one revolution. Thus, the 'Could have' requirement is reached.

Maximum phase error Motor M is the main cause of the maximum phase error, in colatitudinal direction. The maximum speed deviation of Motor M is $0.29\,\%$, with respect to the steady-state speed. This corresponds to a maximum phase error of $1.044°$ in one revolution. Therefore the 'Could have' requirement on phase error is reached (phase error $< 5°$).

Colour The colour of the projection is red monochrome light with a wavelength of $650\,\mathrm{nm}$. Therefore the 'Must have' requirement is reached. For this project, a monochrome light source is enough to create satisfying results and give a proof of concept.

SH order The software has currently been developed for spherical harmonics of orders 0, 1 and 2. However, due to some bugs in the software, only one of these can be projected. At the moment this is the function of order 2 and index -2.

Also, some unfinished work relating to the Hall switches give rise to some synchronisation issues, which cause double projections at different orientations.

When these are fixed, the device will be able to project all the specified spherical harmonics correctly. When this has been done, the 'must have' requirement can be fulfilled.

Brightness The prototype is able to capture patterns in a completely dark room. Therefore the 'Must have' requirement is reached. To reach the 'Could have' category, the light source should have a higher light intensity than the ambient light. Then, a camera can capture the pattern in daylight.

Light levels The driver and the microcontroller together allow for 256 light levels ($8\,\mathrm{bit}$), thus the 'Should have' requirement is fulfilled.

Camera synchronisation The microcontroller can synchronise the pattern and the camera to take a photograph. The camera settings are set manually by the user. Thus the 'Should have' requirement is reached. In order for the microcontroller to also control the camera settings, an extra (wireless) connection between the microcontroller and the camera is needed.

User interface A user interface has been implemented via a command line interface using a Python program. It allows the user to control the device intuitively using only four different commands. This means that the 'Must have' requirement is reached.

Price The material costs for the measurement light bulb are roughly €150.

Safety The output power of the used laser is within the TU Delft regulations and is therefore considered safe. The prototype can be controlled wirelessly which eliminates the need of being close to the moving parts of the device when performing measurements. Also, a safety measure has been implemented to make sure that the motors and the laser shut down if something gets stuck in them or a part falls of.

Chapter 9: Conclusion and future work

9.1 Conclusion

The goal of this project was to deliver a proof of concept for the measurement light bulb. The final prototype is able to project a spherical harmonic onto its surroundings. However, the prototype only works in a low light environment. In environments with a higher light intensity, the camera is not able to distinguish the ambient light from the the projected light. Patterns can be uploaded to the prototype using a Bluetooth connection. Also, the control signals, like a starting and stopping signal, are managed by Bluetooth. Although not implemented yet, the prototype could support camera synchronisation, to capture the illumination impact of the measurement light bulb.

9.2 Future work

All requirements for the prototype were reached to some extent (Must have/Should have/Could have), yet there are still things to improve on for future versions of the measurement light bulb. This prototype is only used for a proof of concept. A future design for a measurement light bulb could improve on individual subsystems as well as the system as a whole.

Beam profile The current beam profile has a quasi-Gaussian distribution. A future version of the measurement light bulb could contain a laser with a more accurate Gaussian distributed profile or a circularly symmetric beam profile. This will reduce errors in the projections or omit the need for complicated compensation algorithms for this problem.

Light output intensity The current prototype is only able to capture spherical harmonic projections in a completely dark room. A future model could contain a light source with a higher power output. This would enable the measurement light bulb to perform measurements in lit rooms as well as dark rooms. However, this would require the involvement of a laser safety officer.

Spectrum of the light source The current prototype of the measurement light bulb can only emit red light with a wavelength of $650\,\mathrm{nm}$. A future design of the measurement light bulb could improve on this by using a light source that covers the complete visible light spectrum or even a light source that can cover certain parts of the spectrum upon request.

Linearity of light source As seen in tests, the light intensity as captured with the camera is not completely linear with the PWM signal that was fed to the laser driver. A future model of the measurement light bulb could contain a linear laser driver or could compensate for this problem using software.

Camera The Canon EOS 5D Mark II has two main forms of unpredictable delay. Firstly the shutter delay, which is the time between the signal that activates the camera to take a picture and the opening of the shutter. Secondly the buffer delay, which is the time between the end of one exposure and the start of the next, needed for saving the image file. To implement an accurate and efficient camera synchronisation

algorithm, a camera with predictable delays is required. In addition, newer camera models often have better image sensors that have better low-light performance, which would give more accurate results.

Light levels Together with the microcontroller, the laser driver is able to output 256 different light levels (8 bit). The sensor of the camera is able to capture 16384 (14 bit) different light levels. Therefore, in a future model of the measurement light bulb, the amount of light levels could be increased up to 16384 (14 bit), equal to the sensitivity of the sensor in the camera.

Construction Although the construction is functional, a few aspects could be improved. Motor B, its corresponding and the power converters can be put into a 3D printed box, which can be mounted to the bottom of the current construction. This way there will be no loose wires or components. This box could also have a mounting point for a camera tripod. This way the system could easily be placed in many position. Another possible point of improvement is the part of the projection that is obstructed by the construction. This obstruction could be reduced if the construction is designed differently.

Start-up time The start-up time of the measurement light bulb is currently around a minute, but this could be reduced significantly if the symbol rate of the Bluetooth communication was increased. Currently, this is set at 9600 Bd, but this could be increased to 115 200 Bd or even to 1 382 400 Bd, for a approximate speed-up of 10 or 100 respectively.

Motor speed To reduce the projection time, the time it takes to capture one pattern, the motors could be driven at higher speeds. In this way more measurements could be performed within a shorter amount of time.

Higher order spherical harmonics Future work could include higher order spherical harmonics to be able to be projected. The hardware of the device is already capable of this, but the patterns for higher order have not been calculated and stored. If this were to be done however, they could be projected.

Power supply The current implementation uses two AC/DC converters. One for the stepper motor and one for the rest of the system. In a future version this could be reduced to one AC/DC, by changing the topology of the power supply. Another improvement could be the use of a battery to power the system. It is expected that a large battery pack would be needed in order to power the whole system.

User interface The user interface could be improved by transforming it into a graphical user interface. This allows for more intuitive usage.

Bibliography

Slip ring, 6 wires. Adafruit. URL https://www.adafruit.com/product/736. Accessed: 16-06-2019.

Hall-Effect IC Applications Guide. Allegro MicroSystems, LLC. URL https://www.allegromicro.com/~/media/Files/Technical-Documents/AN27701-Hall-Effect-IC-Application-Guide.ashx. Accessed: 16-09-2019.

Autodesk. Fusion360, 2019. URL https://www.autodesk.com/products/fusion-360/overview. Accessed: 02-06-219.

SL42S247A NEMA 17 bipolar, 1.8° *step*. China. URL https://reprapworld.nl/datasheets/SL42S247A.pdf. Accessed: 16-06-2019.

Dassault Systmes SolidWorks Corp. Solidworks, 2018. URL www.designsolutions.nl/Solidworks. Accessed: 02-06-219.

P. Debevec, T. Hawkins, C. Tchou, H.-P. Duiker, W. Sarokin, and M. Sagar. Acquiring the reflectance field of a human face. In *Proceedings of the 27th Annual Conference on Computer Graphics and Interactive Techniques*, SIGGRAPH '00, pages 145–156, New York, NY, USA, 2000. ACM Press/Addison-Wesley Publishing Co. ISBN 1-58113-208-5. doi: 10.1145/344779.344855. URL http://dx.doi.org/10.1145/344779.344855.

G. F. Franklin, J. D. Powell, and A. Emami-Naeini. *Feedback Control of Dynamic Systems*. Pearson, Upper Saddle River. NJ 07458, 2015.

GreatScott! Make your own POV LED globe. https://www.youtube.com/watch?v=69G522AeRq8, 2017. Accessed: 25-04-2019.

S. Groenendijk. POV globe project. https://www.youtube.com/watch?v=kut4uUSUP94, 2018. Accessed: 26-04-2019.

T. Hawkins, J. Cohen, and P. Debevec. A photometric approach to digitizing cultural artifacts. In *Proceedings of the 2001 Conference on Virtual Reality, Archeology, and Cultural Heritage*, VAST '01, pages 333–342, New York, NY, USA, 2001. ACM. ISBN 1-58113-447-9. doi: 10.1145/584993.585053. URL http://doi.acm.org/10.1145/584993.585053.

M. Ibrahim. Spherical coordinates colatitude longitude clip art. http://www.clker.com/clipart-29223.html.

S.-H. Kim. *Electric Motor Control: DC, AC, and BLDC motors*. Elsevier, Amsterdam, 2017.

M. Levoy, S. Rusinkiewicz, M. Ginzton, J. Ginsberg, K. Pulli, D. Koller, S. Anderson, J. Shade, B. Curless, L. Pereira, J. Davis, and D. Fulk. The digital michelangelo project: 3d scanning of large statues. In *Proceedings of SIGGRAPH 2000*, pages 131–144. ACM, 2000. ISBN 1-58113-208-5.

LTspice. Linear Technology, Analog Devices, 1999. URL https://www.analog.com/en/design-center/design-tools-and-calculators/ltspice-simulator.html. Accessed: 010-06-219.

R. Luger. Basics: Spherical Harmonics Maps. https://rodluger.github.io/starry/v0.3.0/tutorials/basics1.html, 2018.

RS PRO DC motor, 19.68 W. MFA/como drills. URL https://nl.rs-online.com/web/p/dc-motors/2389721/. Accessed: 16-06-2019.

R. Ramamoorthi and P. Hanrahan. An efficient representation for irradiance environment maps. In *Proceedings of the 28th annual conference on Computer graphics and interactive techniques*, pages 497–500. ACM, 2001.

STEPSTICK DRV8825 v1.0 DATASHEET. RepRapWorld B.V. URL https://reprapworld.com/datasheets/datasheet%20drv8825.pdf. Accessed: 8-06-2019.

N. Z. Salamon, M. Lancelle, and E. Eisemann. Computational light painting using a virtual exposure. In *Computer Graphics Forum (Proceedings of Eurographics)*, volume 36. Eurographics, John Wiley & Sons, 2017. URL http://graphics.tudelft.nl/Publications-new/2017/SLE17.

UA78Mxx Positive-Voltage Regulators. Texas Instruments, a. URL http://www.ti.com/lit/ds/symlink/ua78m.pdf. Accessed: 10-06-2019.

UA78xx Fixed Positive-Voltage Regulators. Texas Instruments, b. URL http://www.ti.com/lit/ds/symlink/ua78.pdf. Accessed: 16-06-2019.

LM2679 SIMPLE SWITCHER 5-A Step-Down Voltage Regulator With Adjustable Current Limit. Texas Instruments, 2016. URL http://www.ti.com/lit/ds/symlink/lm2679.pdf. Accessed: 08-06-2019.

B. Tunwattanapong, G. Fyffe, P. Graham, J. Busch, X. Yu, A. Ghosh, and P. Devebec. Acquiring reflectance and shape from continuous spherical harmonic illumination. In *ACM Transactions on Graphics*, volume 32. Association for Computer Machinery, 2013. URL https://dl-acm-org.tudelft.idm.oclc.org/citation.cfm?doid=2461912.2461944.

Cura. Ultimaker, 2019. URL https://ultimaker.com/en/products/ultimaker-cura-software. Accessed: 16-06-2019.

W. Wu. Dc motor parameter identification using speed step responses. In *Modelling and Simulation in Engineering*, volume 2012. Hindawi Publishing Corporation, 2012. doi: 10.1155/2012/189757.

VET24US240C2-JA - AC/DC Power Supply, ITE, 1 Output, 24 W, 24 V, 1 A. XP Power, a. URL https://nl.farnell.com/xp-power/vet24us240c2-ja/adaptor-ac-dc-24v-1a/dp/2708287?st=ac/dc. Accessed: 16-06-2019.

AFM45US12C2 - AC/DC Power Supply, ITE & Medical, 1 Output, 48 W, 12 V, 4 A. XP Power, b. URL https://nl.farnell.com/xp-power/afm45us12c2/adaptor-ac-dc-medical-12v-4a/dp/2063814?st=12v%204a. Accessed: 16-06-2019.

W. Yamada, K. Yamada, H. Manabe, and D. Ikeda. iSphere: Self-luminous spherical drone display. pages 635–643, 10 2017. doi: 10.1145/3126594.3126631.

Appendices

Appendix A: Design choice

In this chapter, several design options will be discussed, the option that was chosen in the end and finally what is to be delivered to achieve this design.

A.1 Design options

At the start of the project, the CGV group proposed a basic idea for an implementation of the measurement light bulb. In addition to this, two alternative implementations were thought of. These three basic implementations could be all solutions to the problem. They all work with one or multiple light sources that spin around to project onto a sphere. The reflections of this light in the room are captured with a camera with a sustained shutter time to capture one or more entire rotations. A brief explanation of the three design ideas is given below, of which the corresponding design impressions can be seen in Figure A.1.

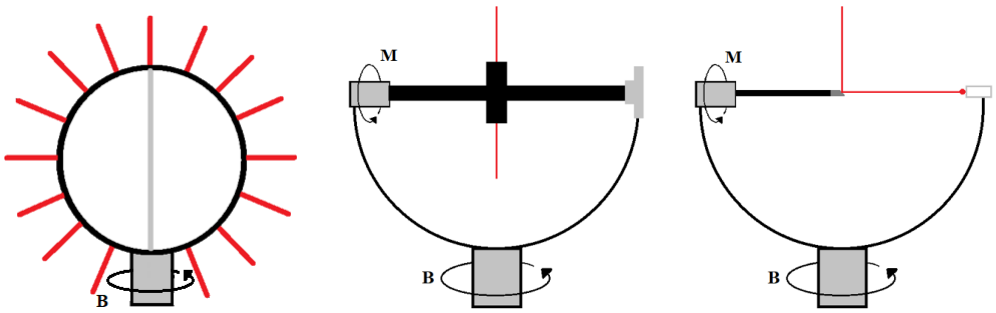

(a) Design 1 (b) Design 2 (c) Design 3

Figure A.1: Sketches of basic design options. Red lines indicate lasers, grey rectangles indicate motors, the letters M and B describe the axes of rotation and the black arrows indicate the direction of this rotation.

Design 1 This design consist of a ring with light sources, which can all be controlled individually at high speed. The ring is rotated around axis B. Due to the rotating movement, the ring projects onto a sphere. By varying the light intensity of the individual light sources during the rotation, the system is able to show light patterns on the sphere.

Design 2 This design consists of one or two light sources that rotate(s) around two perpendicular axes. With the rotation around axis M, the light source(s) will project onto a circle. When this part is rotated around axis B, which is perpendicular to axis M, the device will be able to project onto an entire sphere. By varying the intensity of the light source while the device spins around both axes, it is possible to project different light patterns into a room.

Design 3 This design consists of a rotating mirror instead of a rotating light source. The design uses only one light source that is focused on a mirror that rotates around axis M. In this way the rotating mirror spans up a circle. When this part is rotated around axis B, which is perpendicular to axis M, the device will

be able to project onto a sphere. By varying the intensity of the light source while the device spins around both axes, it will be possible to project different light patterns into a room.

A.2 Design choice

After simulating and testing parts of the designs that are mentioned above the third design was chosen as the best.

Design 1 is not a good option because of a trade-off between weight and resolution. Adding more light sources increases the resolution, but increases the weight, which makes the device heavier to rotate. For a resolution that meets the requirements, this would require a lot of lights, which would be infeasible.

For design 2, axis M was built. Unfortunately it turned out to be very difficult to align the axle of the motor, as it needs to be fixed to the construction on either side. Due to this alignment problem, the laser, which is mounted on axis M, was not able to move smoothly and could not reach the frequency stability that is desired for projecting a stable pattern.

For design 3, a test version of axis M was built, of which the test results were promising. It has the advantage that the only part which is spinning at a high frequency is the mirror, which is relatively light, whereas the laser is only moving slowly. This makes it easier to stabilise the system.

These results and the difficulties with the other two designs, lead to the decision to implement design three.

Appendix B: Motor M parameter estimation and PID tuning

In this chapter, the method used to find the parameters for the Motor M PID controller will be described. In Section B.1 the estimation of the parameters will be discussed. After this the tuning method, using the parameters found in Section B.1, of the PID controller will be discussed in Section B.2.

B.1 Parameter estimation

In order to accurately calculate the PID parameters, a model of Motor M and its load, the mirror mount, is needed. In order to create this model a number of parameters need to be identified. In an ideal case the motor parameters are all stated on the datasheet. However, for most low cost DC motors these parameters are not properly listed in the datasheet. For this reason the parameters were estimated using the method proposed by Wu [Wu, 2012]. The proposed method fits a polynomial to speed measurement data and uses the coefficients of this polynomial to calculate the motor parameters. The method is based on a Taylor series expansion of the theoretical transfer function of a DC motor.
We followed this method to find the motor parameters listed in Table B.1. With these parameters the transfer function of Motor M becomes:

$$\frac{\omega(s)}{V(s)} = \frac{\frac{1}{k_b}}{t_m t_e s^2 + t_m s + 1} \tag{B.1}$$

Where k_b is the back-EMF constant of the motor, t_m is the mechanical time constant, t_e is the electrical time constant and s is the Laplace variable.

Table B.1: Estimated parameters of Motor M

Parameter	Estimated value
k_b	$3.4 \times 10^{-3}\,\mathrm{V\,s\,rad^{-1}}$
t_m	$1.74 \times 10^{-1}\,\mathrm{s}$
t_e	$6.11 \times 10^{-1}\,\mathrm{s}$

Although this model is simplified and the fitted curves did not exactly match the measured data, this transfer function gives us a good starting point to tune the PID constants.

B.2 PID tuning

To tune the PID constants, the estimated transfer function, Equation B.1, was filled into Matlab's PID tuning application. This application calculates PID constants and shows the resulting step response. The PID values that were found using Matlab are $k_P = 7.672$, $k_I = 328.8$ and $k_D = 4.217 \times 10^{-2}$. These constants can not be implemented in the controller immediately, because the speed measurements are done with periods in µs instead of frequencies in Hz. The fastest way to compensate for this was to invert

the signs of the three constants and scale k_I by a factor 10^{-12}. These PID constants were tested by implementing the PID control with the microcontroller and measuring the step response of the system. At first the results were unsatisfactory, so k_I was manually tuned until the response was almost critically damped. The results of this manual tuning are depicted in Figure B.1. The resulting PID values are $k_P = -7.672$, $k_I = -1.4796 \times 10^{-5}$ and $k_D = -4.217 \times 10^{-2}$. These will be implemented in the controller for Motor M.

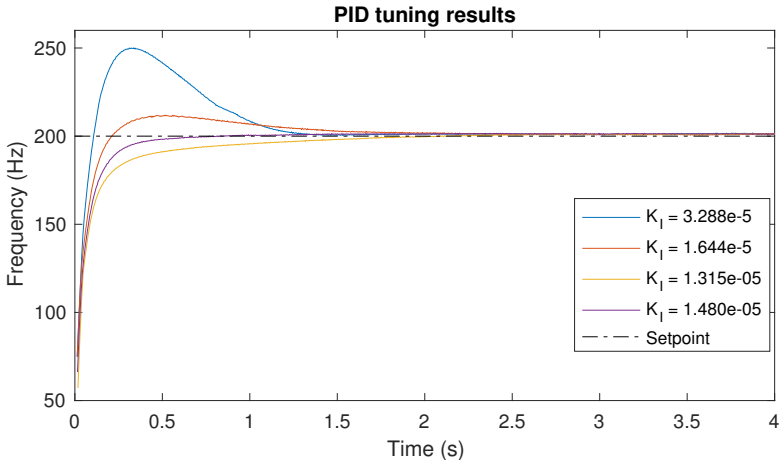

Figure B.1: PID tuning results

Appendix C: Fusion 360 sketches

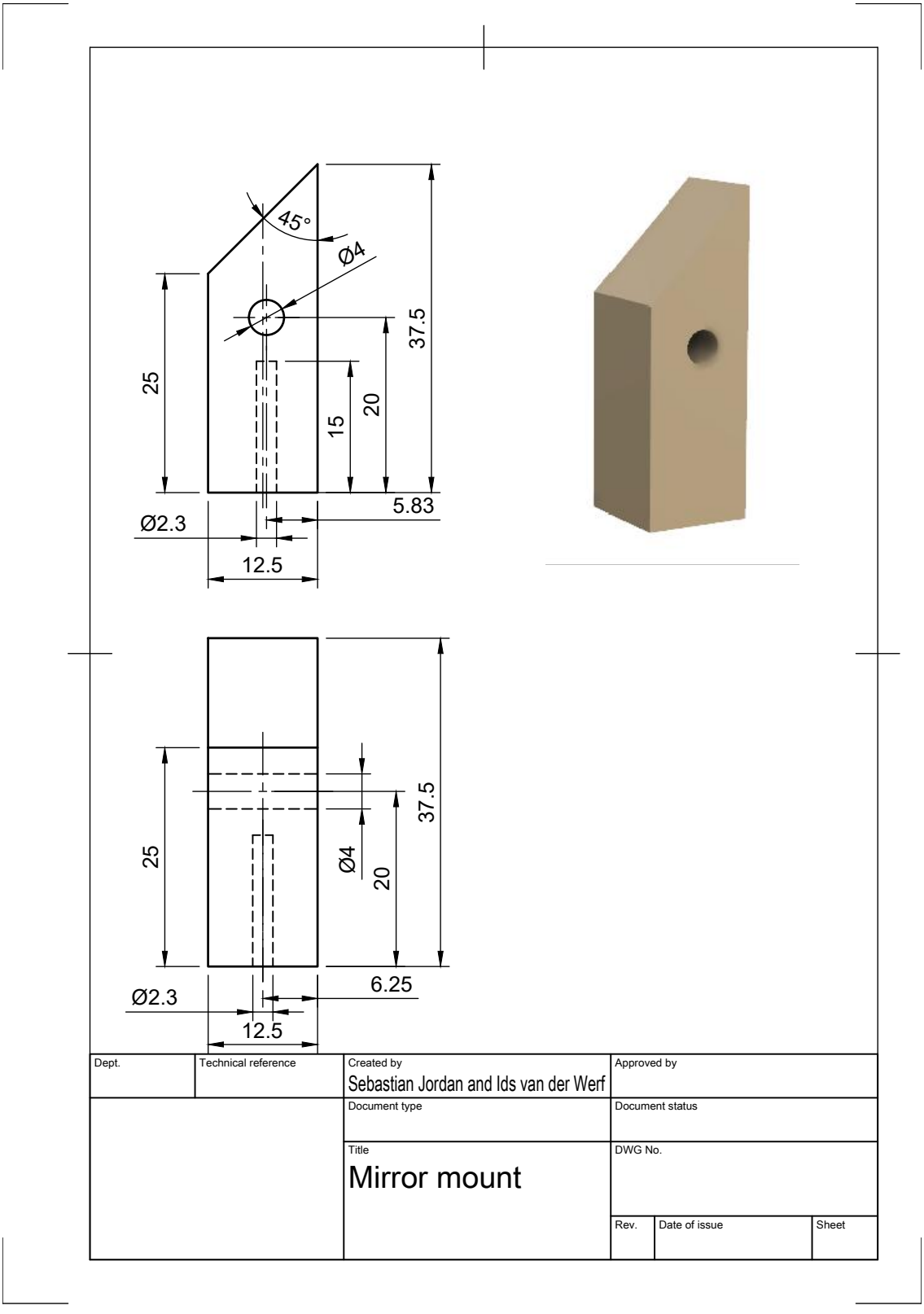

Figure C.1: Technical drawing of the mirror mount

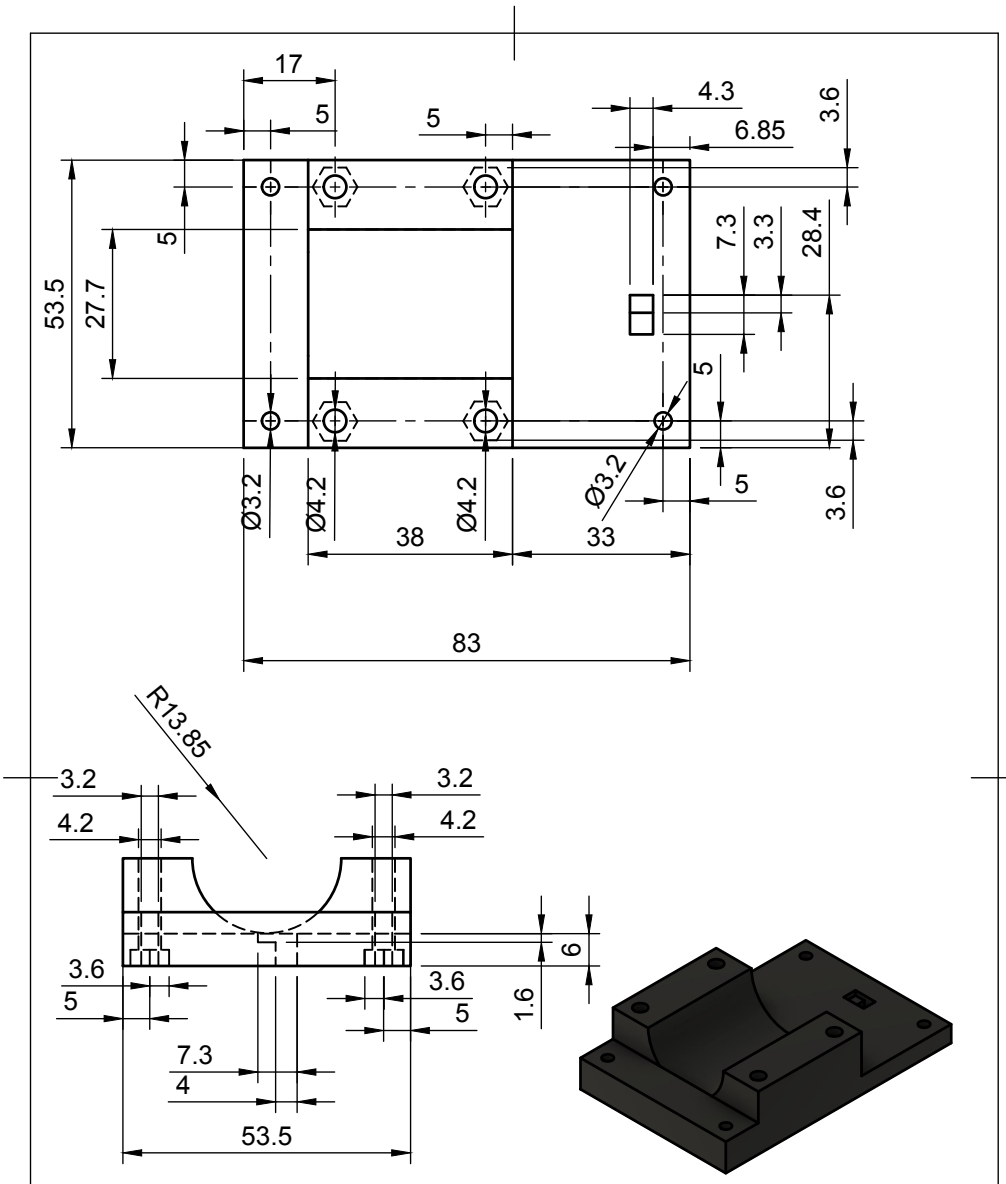

Dept.	Technical reference	Created by Sebastian Jordan and Ids van der Werf	Approved by	
		Document type	Document status	
		Title Motor mount	DWG No.	
			Rev. / Date of issue	Sheet 1/1

Figure C.2: Technical drawing of the mount for Motor M

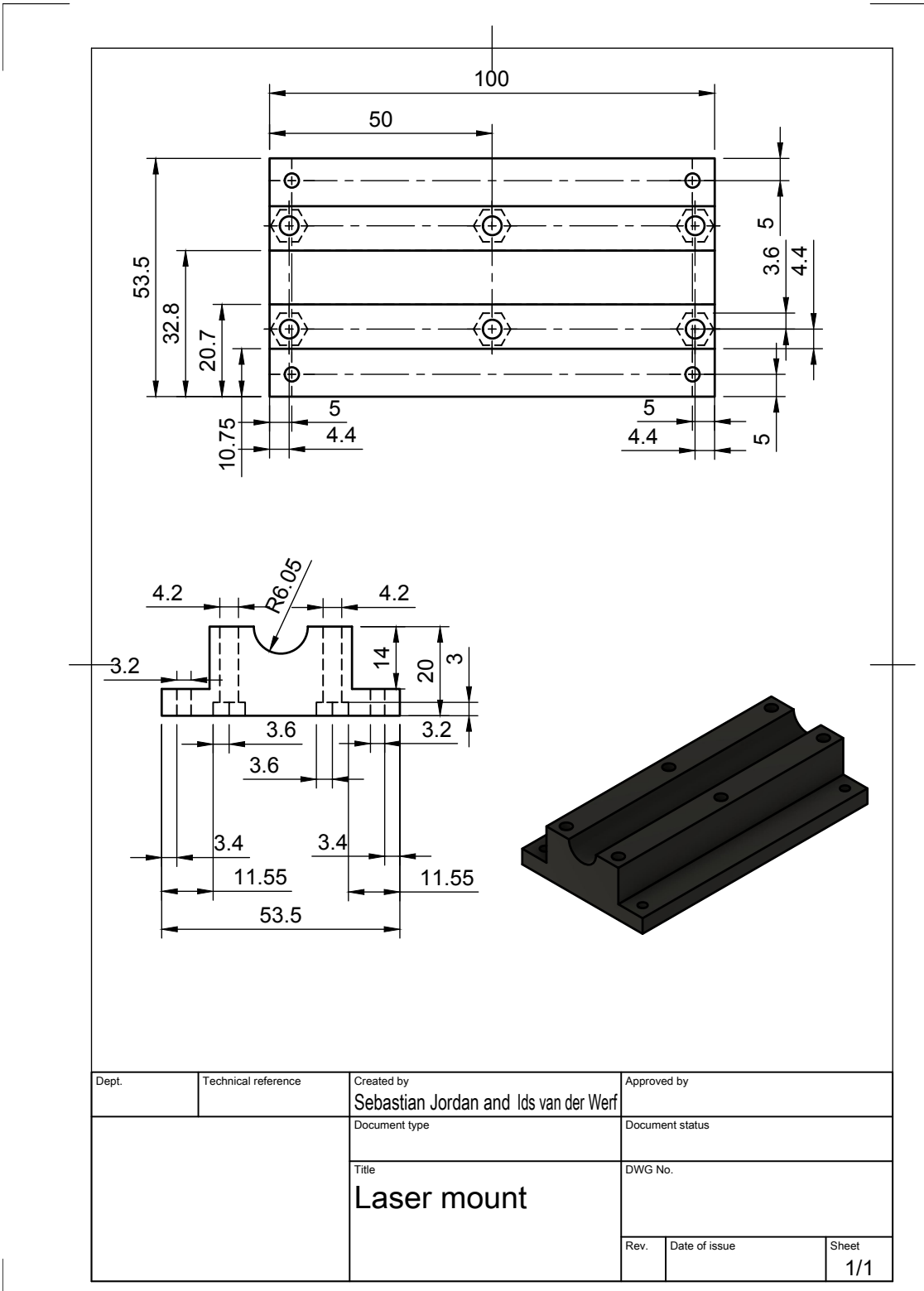

Figure C.3: Technical drawing of the laser mount

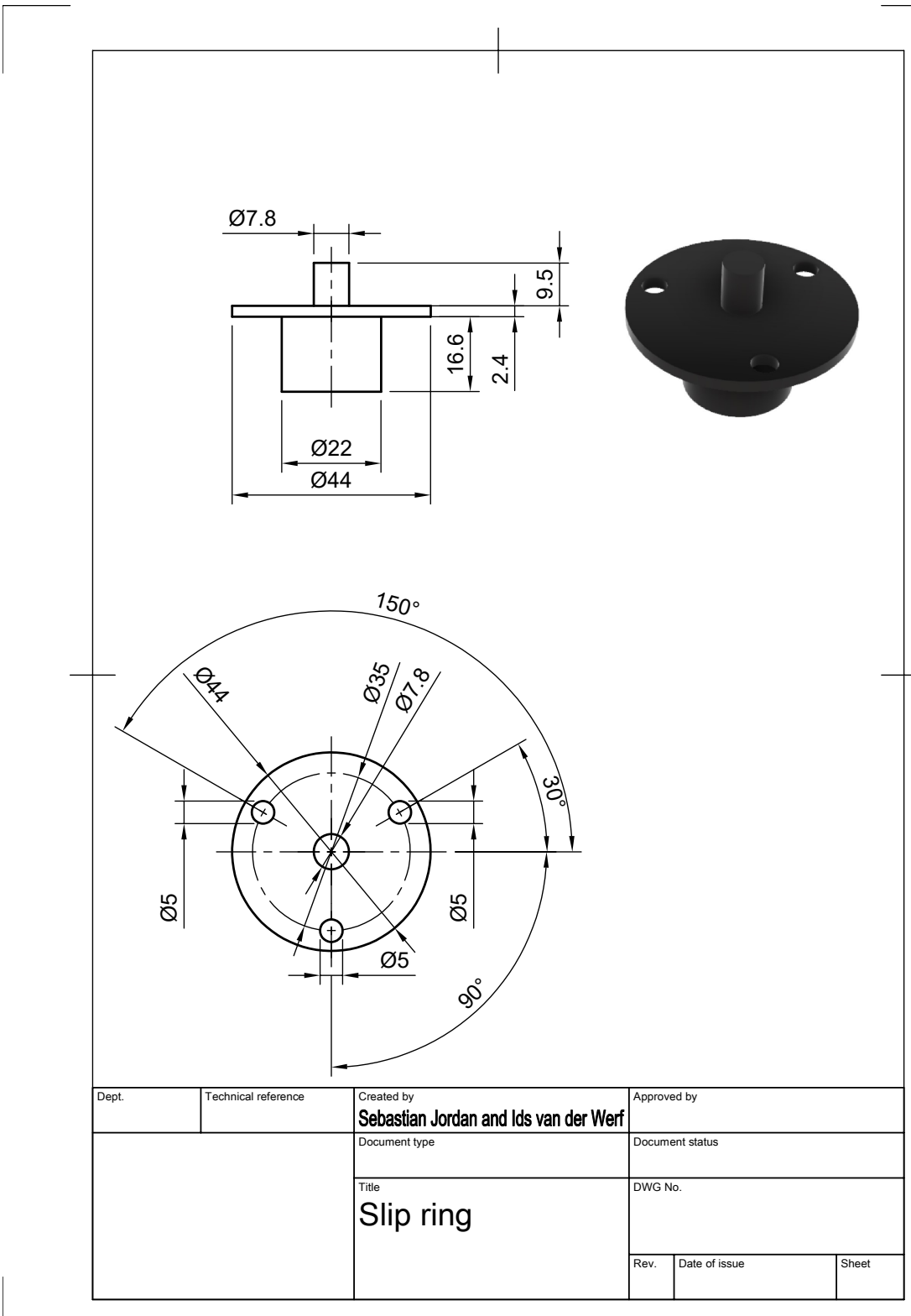

Figure C.4: Technical drawing of the slip ring

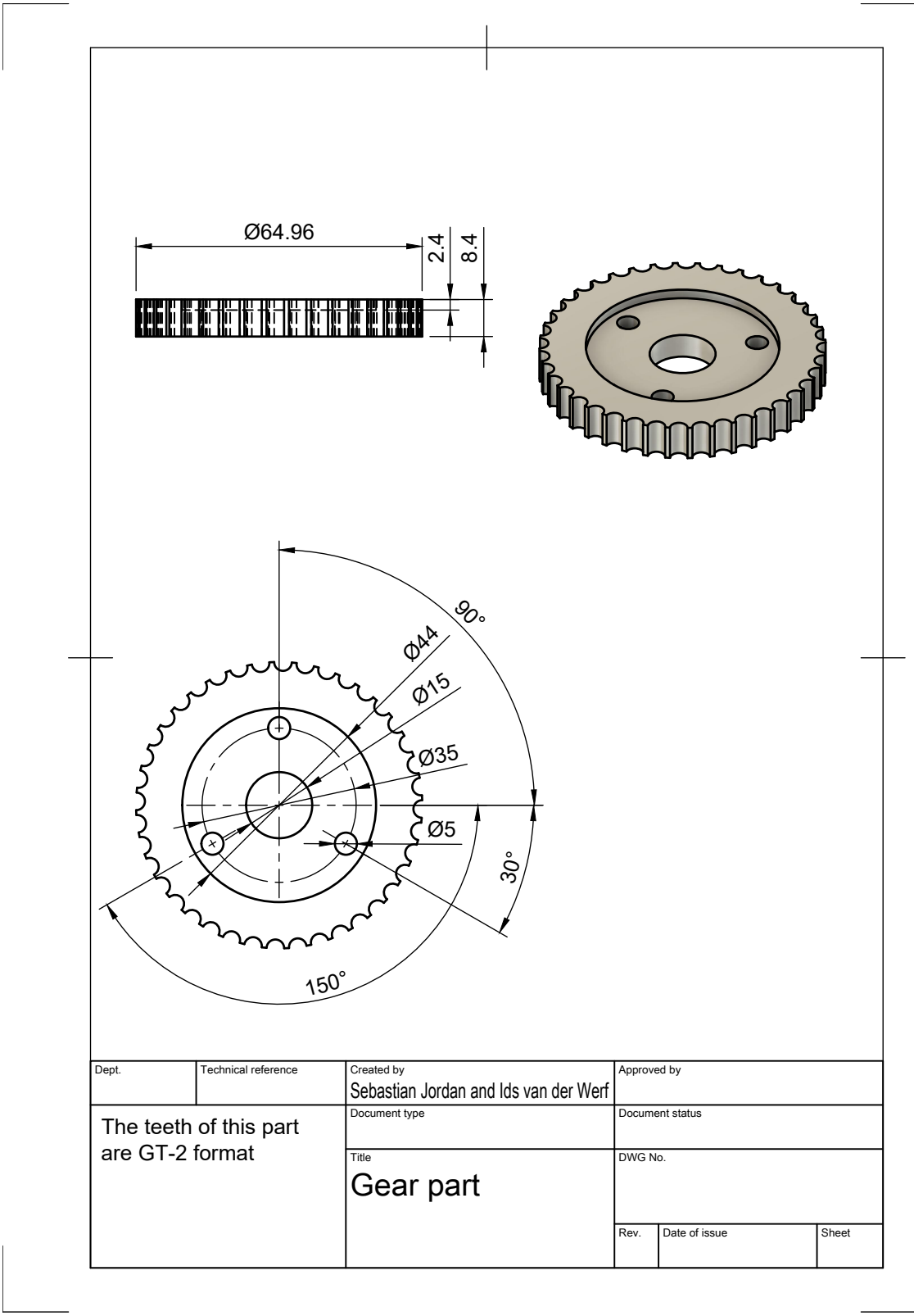

Figure C.5: Technical drawing of the gear part

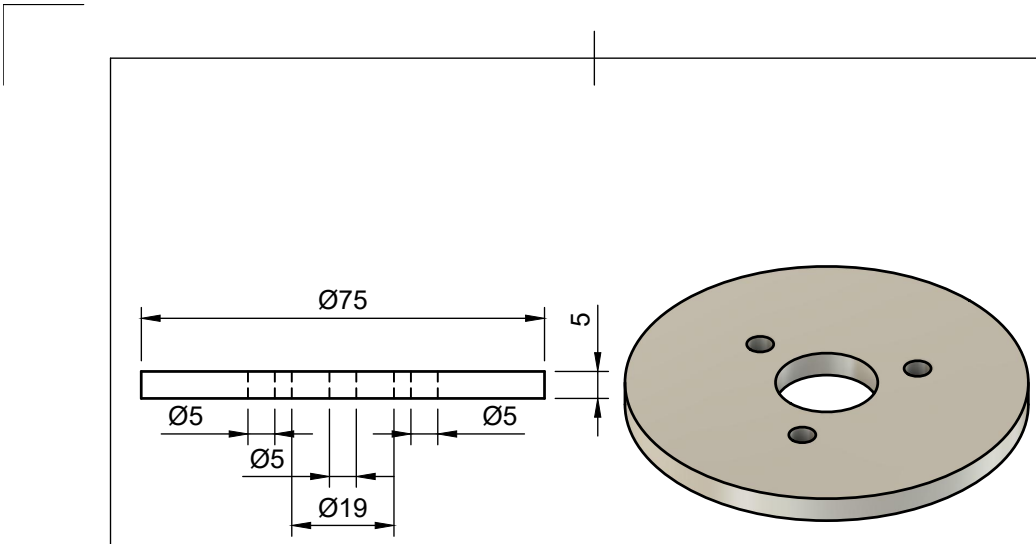

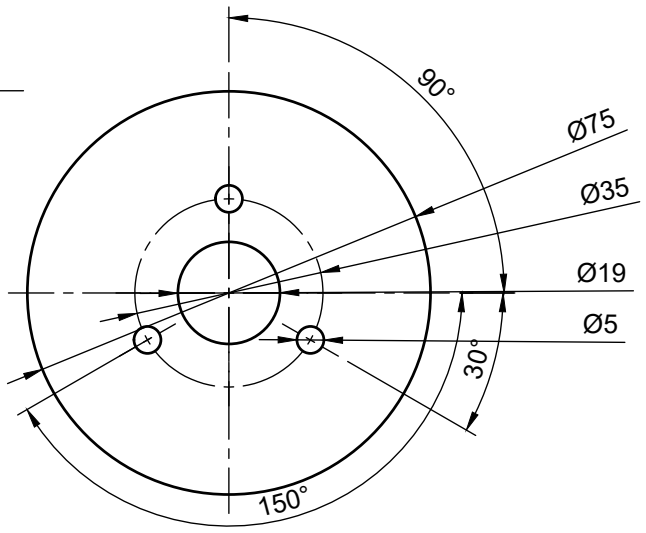

Dept.	Technical reference	Created by Sebastian Jordan and Ids van der Werf	Approved by	
		Document type	Document status	
		Title Flange part	DWG No.	
			Rev. / Date of issue	Sheet 1/1

Figure C.6: Technical drawing of the flange part

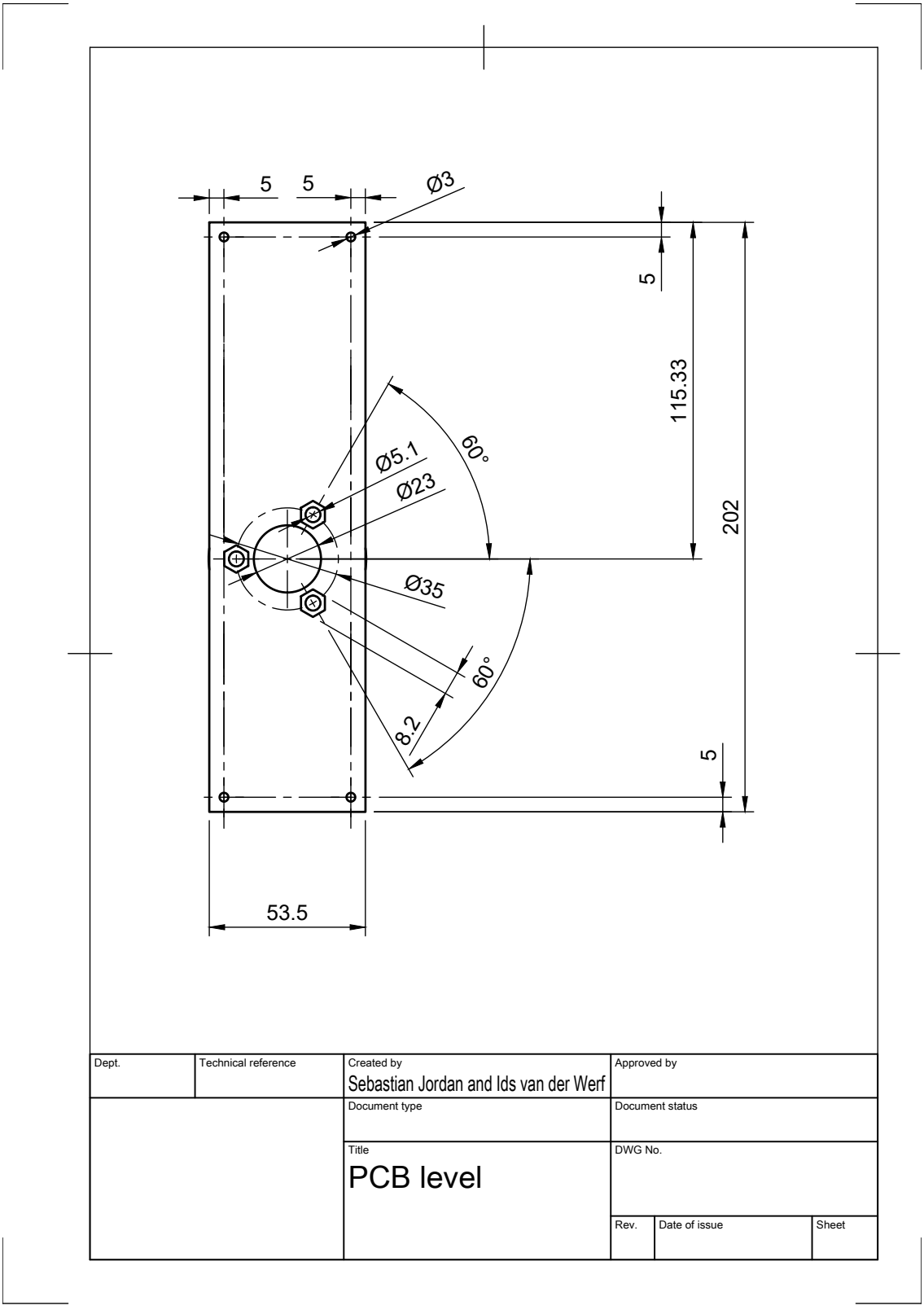

Figure C.7: Technical drawing of the PCB level

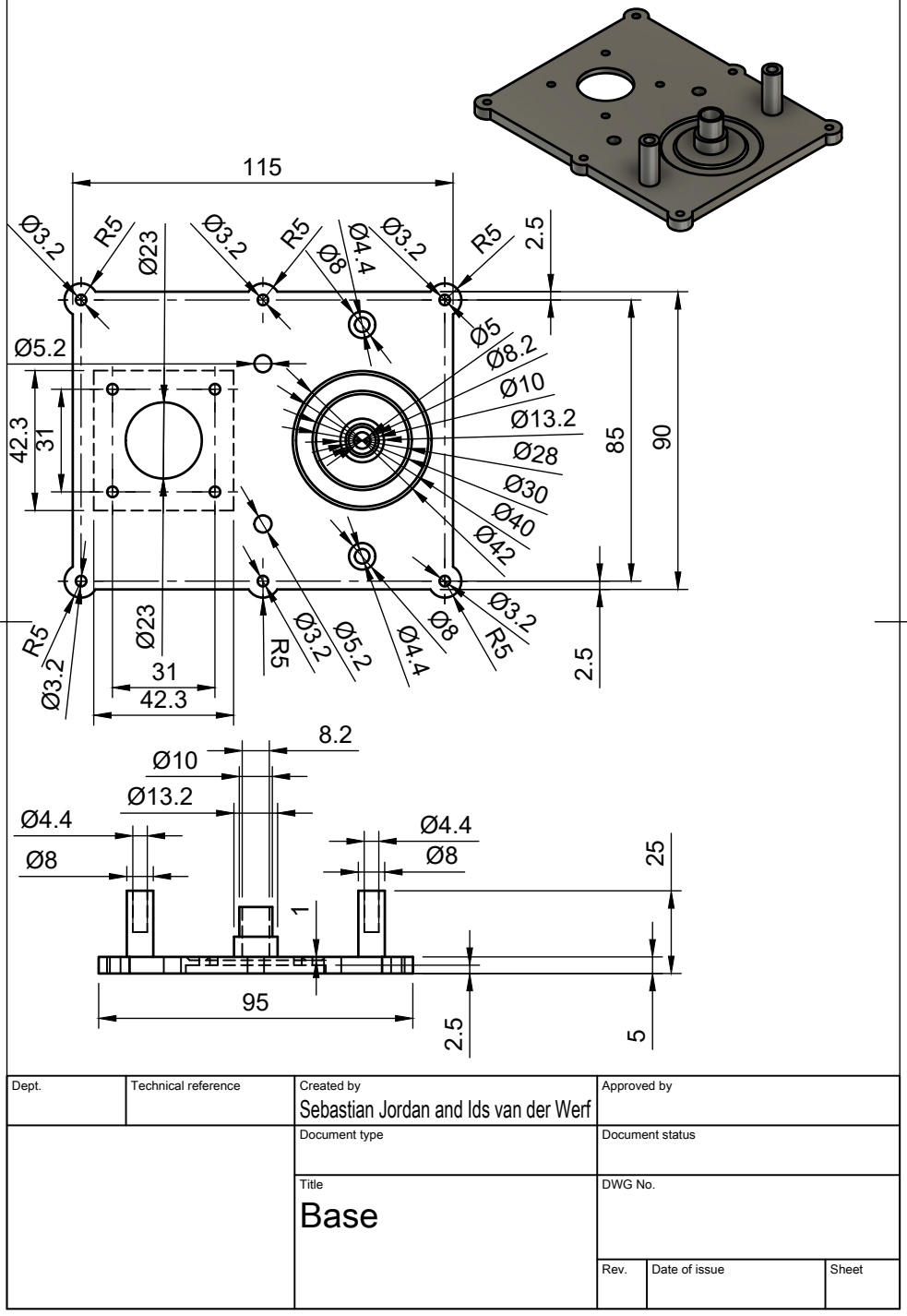

Figure C.8: Technical drawing of the base

Appendix D: Slip ring measurement

The slip ring is the component that connects the electrical wires for one rotating part to a relatively stationary part of the device. The speed of the rotating part should be tested to achieve the highest possible rotations per minute (rpm). By the manufacturer it is rated on 300 rpm [Ada].

Some testing is required to find out if the ring can take more than its original rating. The signal transfer characteristics for the slip ring are unknown. Especially when exceeding the manufacture rating, a test is required to be sure the signals are able to transfer over the slip ring without too much noise.

D.1 Setup

On the axle of a motor a PVC tube is connected. In this tube an oscillator is mounted to generate a signal. Power is transmitted through the slip ring to the oscillator, of which the output is sent back through the slip ring to measure with an oscilloscope. This setup is depicted in Figure B.3.

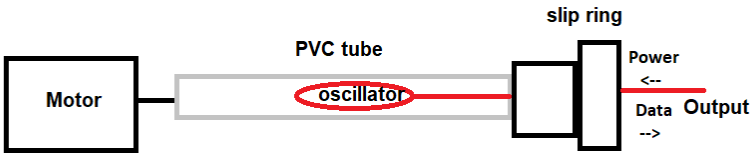

Figure D.1: Schematic view of the test set up

The tube will now rotate when the motor starts and so does one half of the slip ring, whereas the other half will stay stationary and measurable for an oscilloscope.

The oscillator in the tube is constructed around an 555NT timer [1] and the circuit is shown in Figure D.2[2].

D.2 Testing

The testing will be done by changing the speed of the motor and measuring the output signal of the slip ring. By comparing the behaviour of the measured signal and the steady state signal the quality of signal transfer can be determined.

Another possible problem is the heat that might be generated inside the slip ring when it is spinning at a high frequency. After a measurement it should be sensed if the slip ring got heated up.

[1] *Datasheet NE/SA/SE555/SE555C Time*. Philips. `http://pdf.datasheetcatalog.com/datasheet/philips/NE_SA_SE555_C_2.pdf`. Accessed: 01-05-2019

[2] *The simplest 555 oscillator circuit*. `http://www.555-timer-circuits.com/simplest-555-oscillator.html`. Accessed: 01-05-2019

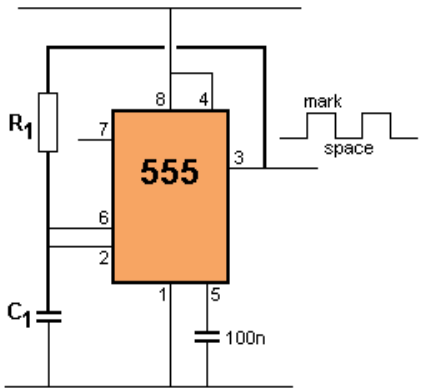

Figure D.2: Schematic of 555t based oscillator.

D.2.1 Results

The result of the measurement at $3750\,\mathrm{rev\,min^{-1}}$ is shown in Figure D.3. As a reference, the signal was also measured at $0\,\mathrm{rev\,min^{-1}}$. This result and the difference between the to results is also shown in Figure D.3. The only spikes in the 'difference' graph have widths around $50\,\mathrm{ns}$. Delays of the slip ring would thus be in the order of nanoseconds (if these spikes are not due to measurement errors).

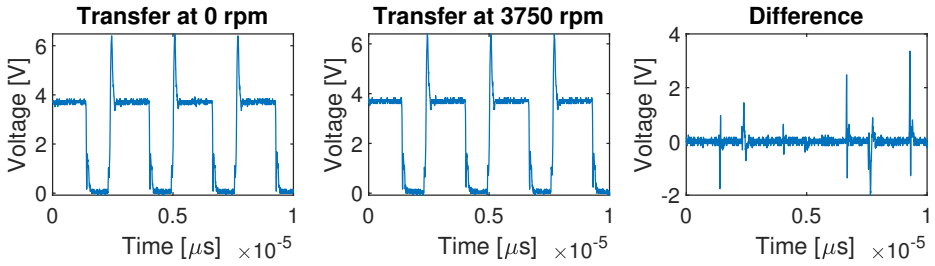

Figure D.3: Results of the slipring measurement

After the measurement, the slip ring was touched to see if spinning it at a much higher rpm than rated had heated it up. However, it was still cold to touch, indicating that there is no mechanical strain on the ring.

D.2.2 Conclusion

The conclusion of this experiment is that the slip ring performs very well under the testing conditions,it shows good performance, even at speeds much higher than its ratings. No noticeable decay in signal quality or noise figure was detected and the slip ring did not get hot. Also an implementation with a slipring is a lot faster than a wireless implementation, which has delays orders of magnitude higher.

Appendix E: Component selection for 7.2 V converter

This chapter describes the calculation and the motivation for all the component values of the 7.2 V DC/DC converter circuit, shown in Figure E.1. The order in which the component values are calculated and their corresponding equations are based on the information given in the datasheet of the switching regulator LM2679 [Tex, 2016], that is used in this circuit.

Resistor R_{16} and R_{18}

These resistors define the output voltage of the converter as shown in Equation E.1. The datasheet suggests using a 1 kΩ resistor for R_{16}. Since the goal for this circuit to have an output voltage V_{out} of 7.2 V and the typical value of V_{FB} equal to 1.21 V, the value of R_{18} can be calculated using Equation E.2.

$$V_{out} = V_{FB} \cdot \left(1 + \frac{R_{18}}{R_{16}}\right) \tag{E.1}$$

$$R_{18} = R_{16} \cdot \left(\frac{V_{OUT}}{V_{FB}} - 1\right) = 1\,\text{k}\Omega \cdot \left(\frac{7.2\,\text{V}}{1.21\,\text{V}} - 1\right) \approx 4.95\,\text{k}\Omega \tag{E.2}$$

Inductor L_1

To determine the inductor value, a nomograph, given in the datasheet [Tex, 2016], is used. First the product $E \cdot T$ [V · µs] has to be calculated using Equation E.3.

$$\begin{aligned} E \cdot T &= \left(V_{IN(MAX)} - V_{OUT} - V_{SAT}\right) \cdot \frac{V_{OUT} + V_D}{V_{IN(MAX)} - V_{SAT} + V_D} \cdot \frac{1000}{260} \\ &= (12\,\text{V} - 7.2\,\text{V} - 0.42\,\text{V}) \cdot \frac{7.2\,\text{V} + 0.5\,\text{V}}{12\,\text{V} - 0.42\,\text{V} + 0.5\,\text{V}} \cdot \frac{1000}{260} = 10.74\,\text{V} \cdot \mu\text{s} \end{aligned} \tag{E.3}$$

This calculated $E \cdot T$ value corresponds to a 15 µH inductor. However, the datasheet states that the use of this value is not practical, because with such an inductor it would be impractical to select correct output capacitors later in the design process. For this reason the suggested 33 µH inductor was chosen.

Capacitor C_{27}

Using the chosen inductor value and the required output voltage, the suggested capacitor for C_{27} is read from a table in the datasheet. For this project, two 100 µF capacitors are needed to handle the load current, which is 3.5 A for this project.

Capacitor C_{23}

Using the chosen inductor value and the required input voltage, the suggested capacitor for C_{23} is read from a table in the datasheet. For this project, two 100 µF capacitors are needed to handle the load current.

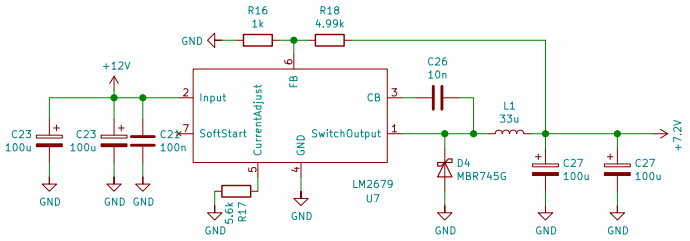

Figure E.1: 7.2 V converter circuit

Table E.1: Overview of the components used for the 7.2 V converter circuit

Component	Type or Value
R_{16}	1 kΩ
R_{17}	5.6 kΩ
R_{18}	4.99 kΩ
C_{21}	100 nF
C_{23}	100 µF
C_{26}	10 nF
C_{27}	100 µF
L_1	33 µH
D_4	MBR745G
U_7	LM2679

Diode D_4

The diode must be able to handle the maximum load current and its reverse voltage rating should be greater than the maximum input voltage. With these two parameters a suggested diode can be read from a table. For this project the maximum input voltage is 12 V. A schottky diode, the MBR745G, suffices.

Capacitor C_{26}

This capacitor is used to improve the efficiency by minimising the power loss during the time the switch is ON. We chose a 100 nF, 50 V capacitor for C_{27}, as recommended in the datasheet.

Resistor R_{17}

The value of resistor R_{17} can be calculated using Equation E.4, that was given in the datasheet (including the value 37.125). This resistor is used to set an output current limit at a suggested value of 6 A. "This allows the use of less powerful and more cost-effective inductors and diodes" Tex [2016].

$$R_{17} = \frac{37.125}{I_{limit}} = \frac{37.125}{6.3\,\text{A}} \approx 5.6\,\text{k}\Omega \tag{E.4}$$

Capacitor C_{21}

This capacitor is used as decoupling/bypass capacitor. In the datasheet of the LM2679 a reference can be found to a document[1] about PCB layout guidelines. This document states: "For high-speed devices (for example, LM267x) do not omit placing input decoupling/bypass ceramic capacitor (0.1 µF-0.47 µF).". For this reason a 0.1 µF ceramic capacitor was used for C_{21}.

[1] *AN-1229 SIMPLE SWITCHER PCB Layout Guideline.* , Texas Instruments. `http://www.ti.com/lit/an/snva054c/snva054c.pdf`. Accessed: 4-06-2019.